Issues related to ocean colour in coastal zones and inland waters

Stewart Bernard, Tim Moore, Stefan Simis, Lisl Robertson, Hayley Evers-King,
Mark Matthews, and Mark Dowell

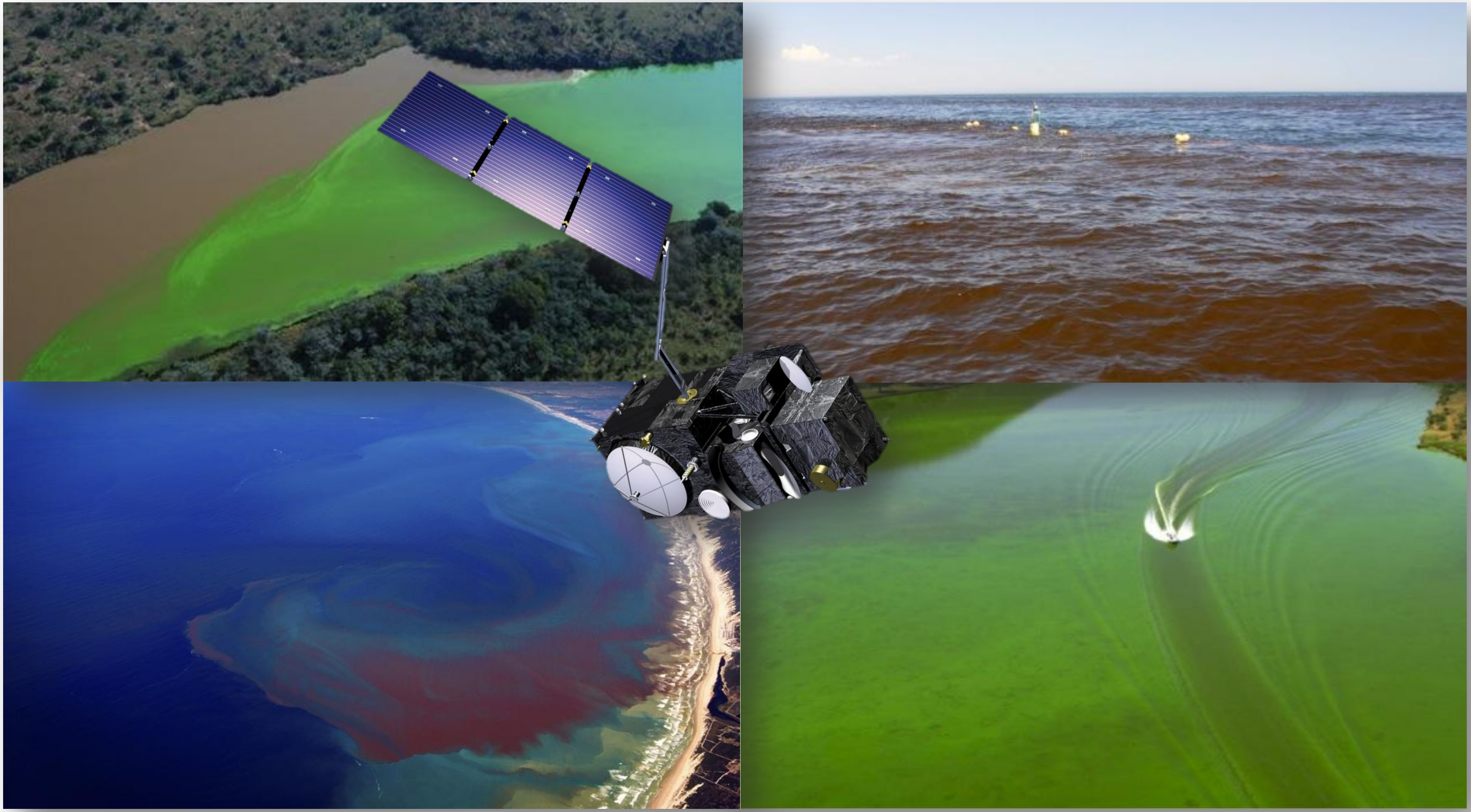

International Ocean Colour Science Meeting, Darmstadt, May 2013

Issues related to ocean colour in coastal zones and inland waters

- Quick summary of some example coastal and inland systems with regard to temporal scales of variability and range of optical complexity
- Harmful algal blooms and some conceptual thinking
- Signal characterisation for Case 2 and eutrophic water types
- Coupled radiative transfer models: better understanding constituent contributions to the ocean colour signal for eutrophic and optically complex waters
- Validation in eutrophic and optically complex waters: challenges and needs
- The atmospheric correction: algorithms to circumvent the pain
- Consideration of algorithm types and structures: regional examples and scaleable algorithm structures
- A few thoughts on the way forward…

Characterising ecological and bio-optical variability for example coastal and inland systems

Several example ecosystems are briefly examined – systems that encompass much of the ecological and optical complexity from global coastal and inland water bodies.

- What are the main temporal scales of variability from an ecological perspective?
- What range in optical complexity in time and space can be expected?
- How does this translate into ocean colour user requirements needed to resolve ecological variability of the systems from the event to longer time scales?

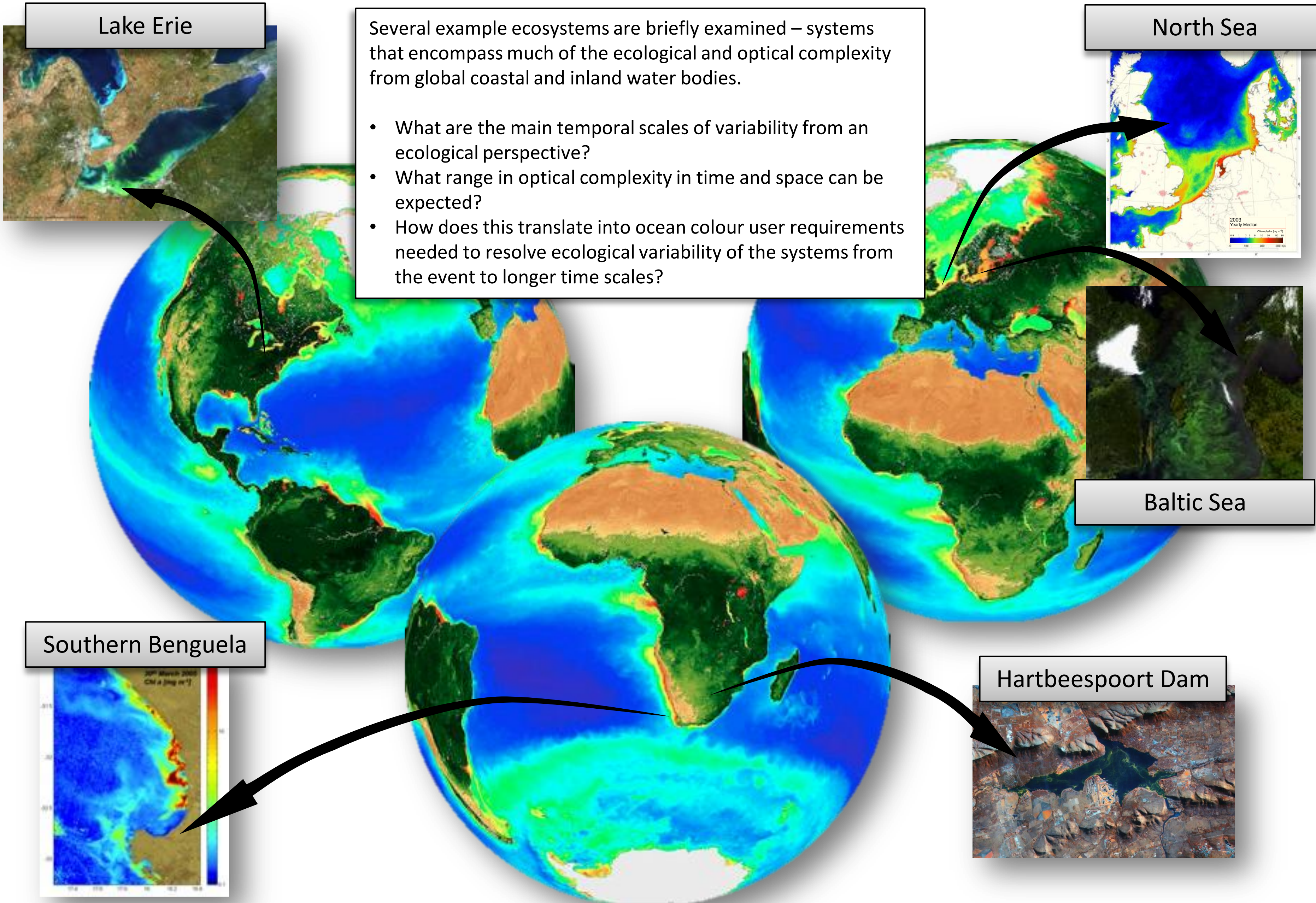

The southern Benguela: a dynamic, productive, phytoplankton dominated upwelling system

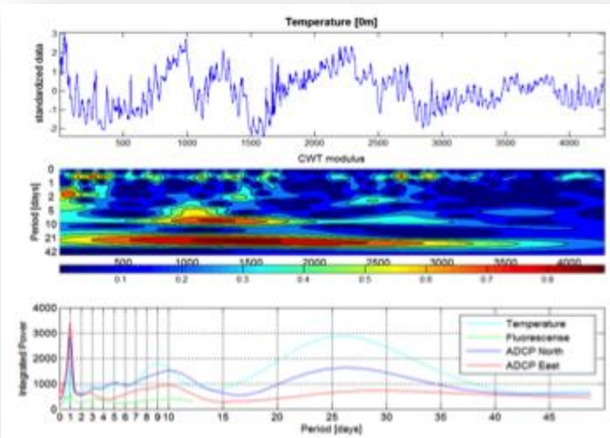

Inertial & 3 -5 day wind driven event scale variability. Fawcett, 2006.

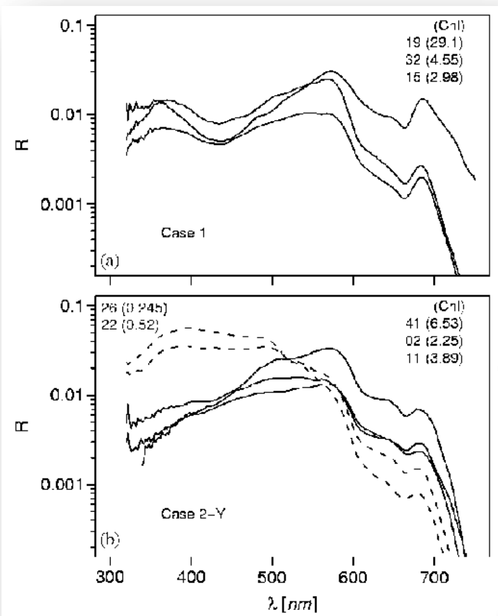

Fig. 10. Irradiance reflectance spectra for some selected stations. (a) Case 1 waters, (b) Case 2-Y waters, and mesotrophic waters (dashed curves). The station numbers and (Chl) are indicated and ordered from top to bottom as the spectra.

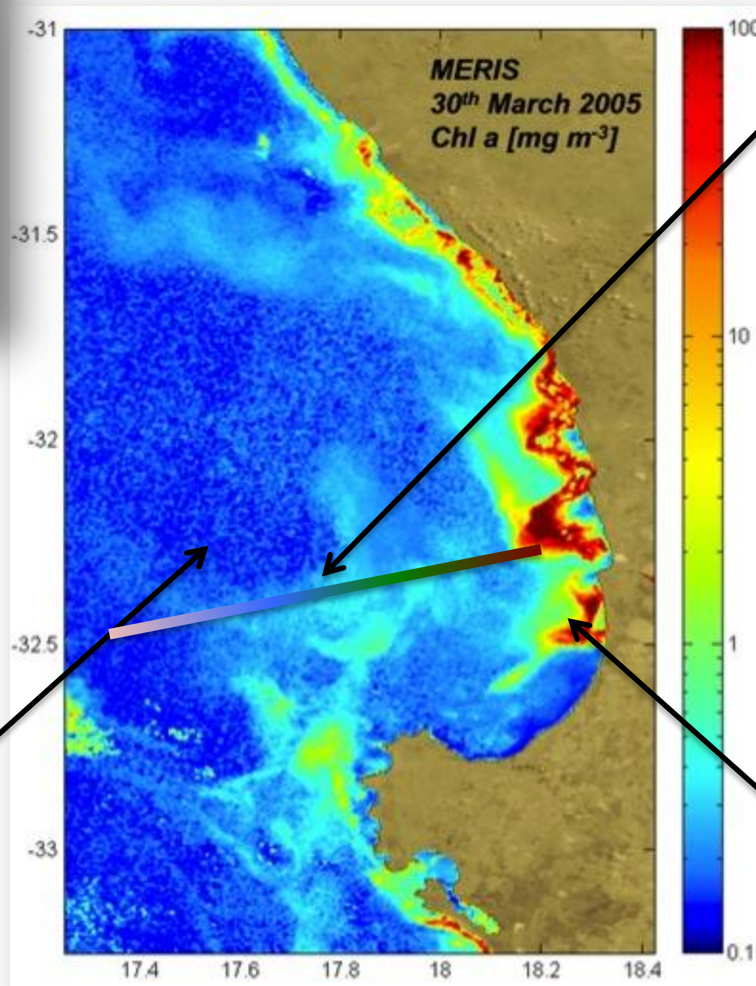

Oligo – to mesotrophic shelf waters with some gelbstoff influence. Morel et al, 2006.

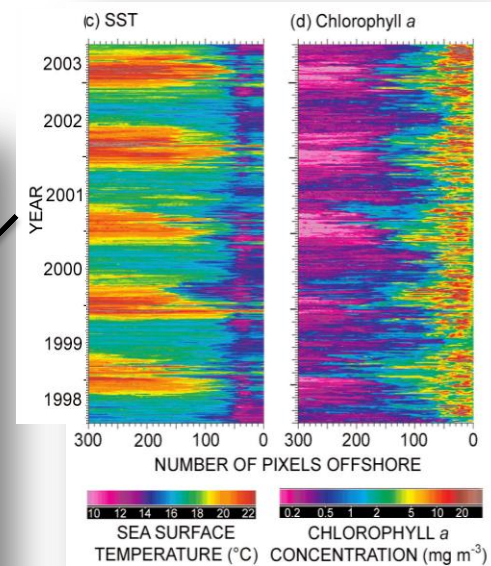

Sub-weekly pulsed event scale dominates summer upwelling season. Weeks et al, 2006.

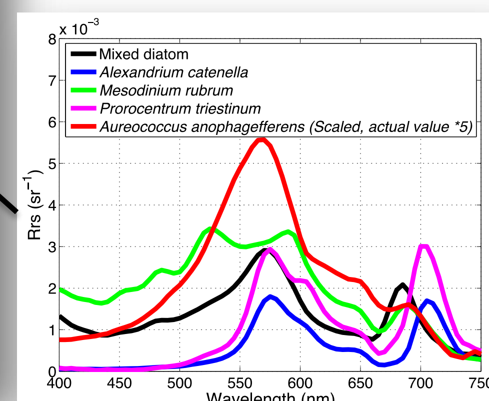

Variety of high biomass blooms in high nitrogen, retentive inshore waters. Bernard et al, in press.

The southern Benguela: a dynamic, productive, phytoplankton dominated upwelling system

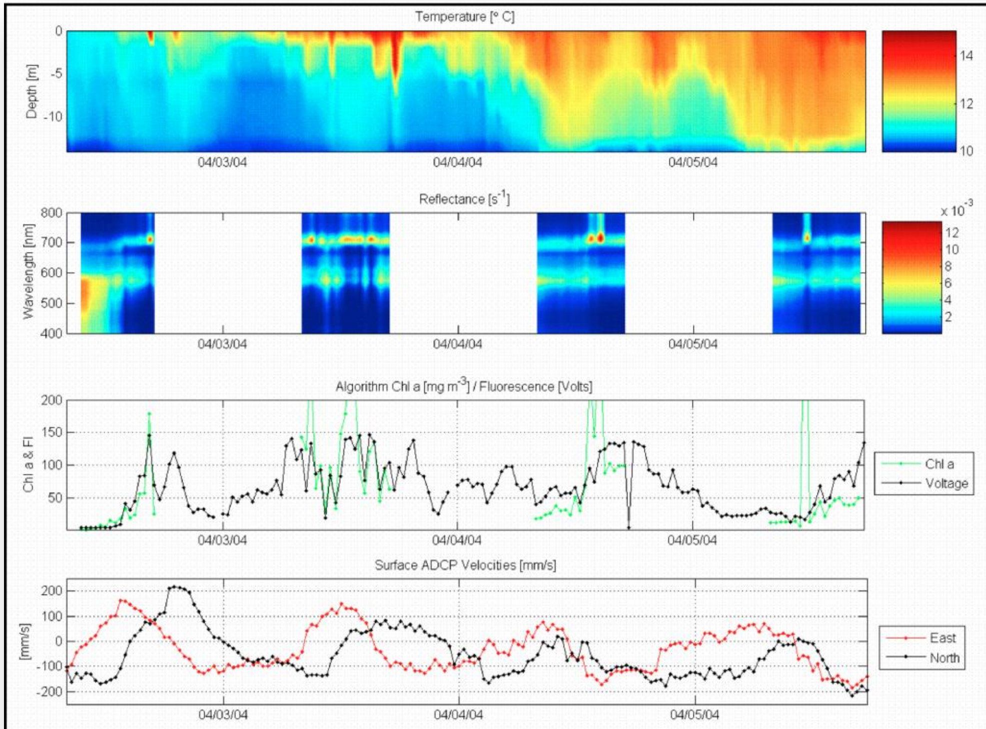

Mooring time series data and MERIS chlorophyll a data showing the detection and wide spatial extent of a bloom of the small dinoflagellate Prorocentrum triestinum from 2nd to 5th April 2004, in the Namaqua shelf region. The bloom appears at the mooring ~ 4 hours after the satellite overpass, as a thin lens of warmer high biomass bloom waters are advected shorewards in the easterly surface flow. Satellite chlorophyll a data, derived through an experimental red band algorithm designed for high biomass application, show the widespread and complex distribution pattern of the bloom. Bernard et al, 2006

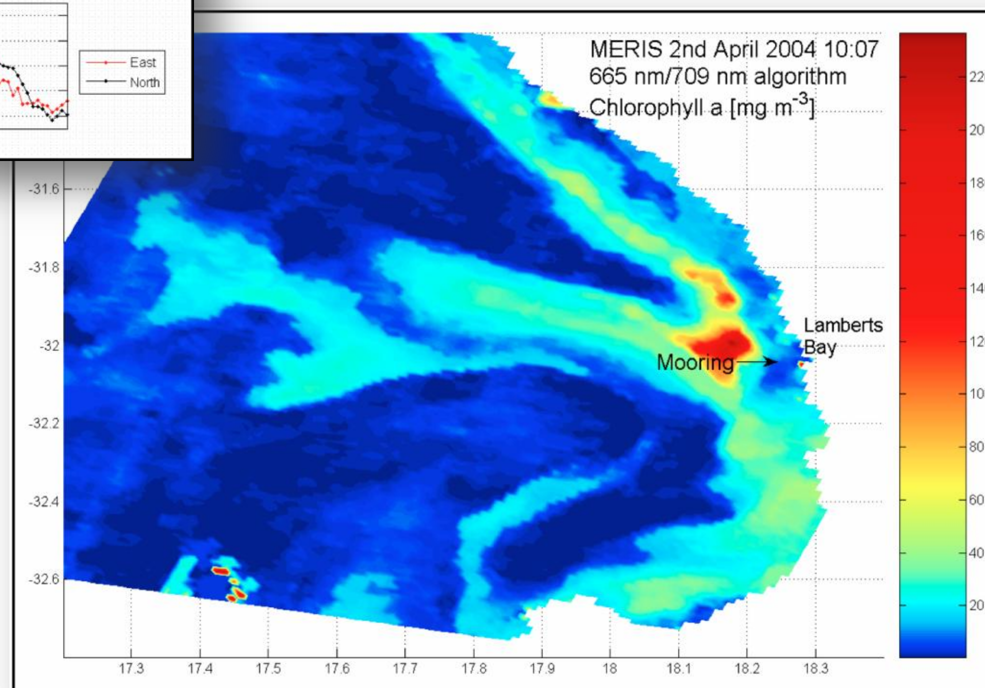

The Baltic Sea: from gelbstoff to cyanobacteria in a semi-enclosed brackish system

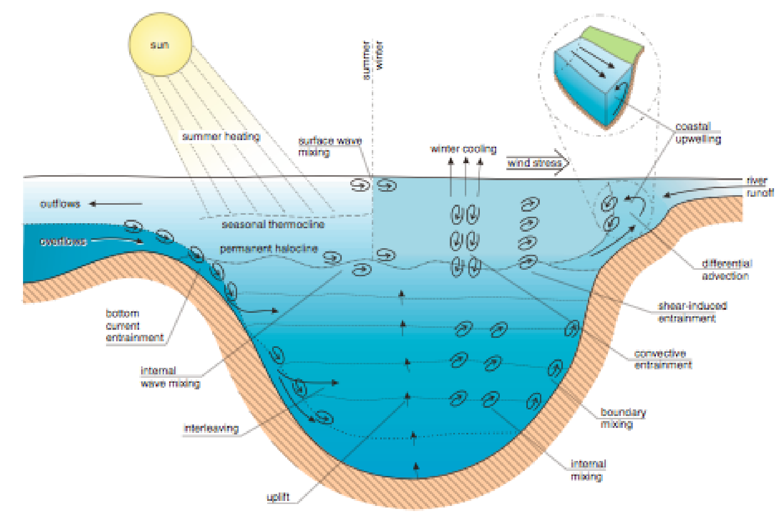

Fig. 2. Scheme of vertical mixing and transport processes in the Baltic Sea.

Complex drivers of inflow & entrainment effects on vertical mixing & stratification, combined with coastal upwelling. Reismann et al 2009, Lips & Lips 2012

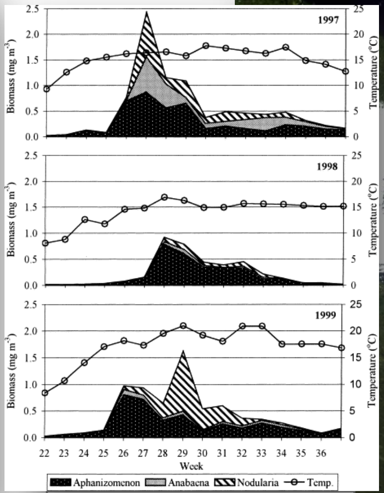

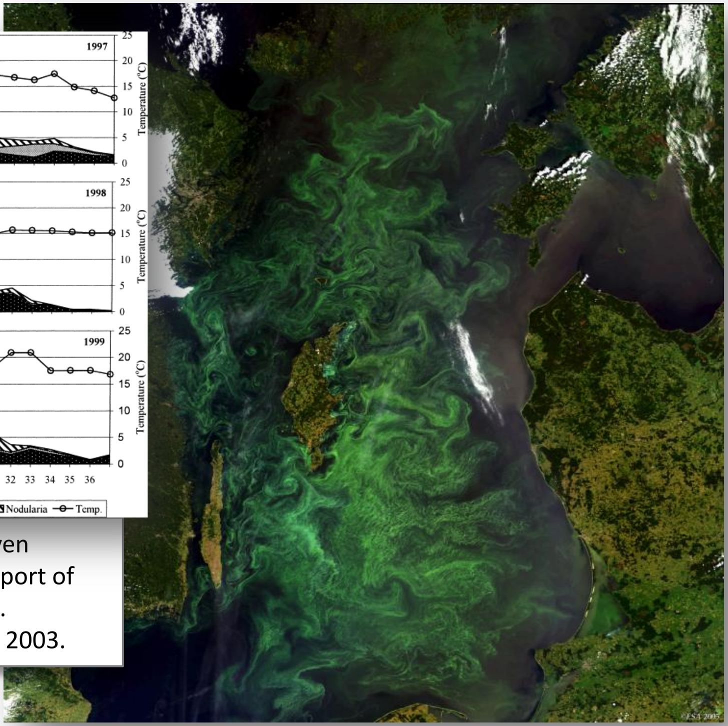

Rapid wind driven advective transport of surface blooms. Kanoshina et al 2003.

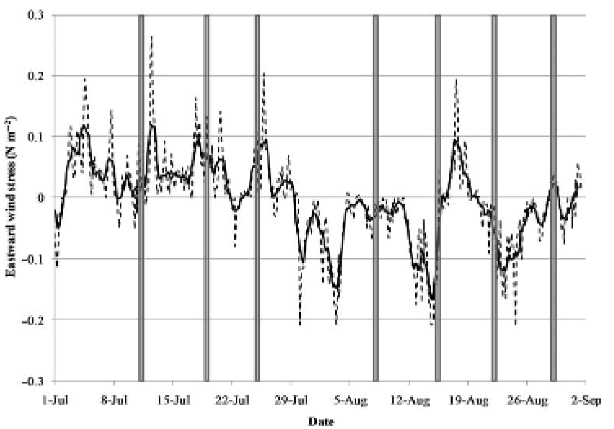

Fig. 2. Eastward wind stress (dashed line) in July–August 2006 estimated using wind data from Kalbådagrund meteorological station. Daily average wind stress is shown as the solid line and vertical grey areas indicate the periods of sampling.

Sub weekly summer wind forcing and frequency of coastal upwelling. Lips & Lips 2012, Lehman et al 2012

The Baltic Sea: from gelbstoff to cyanobacteria in a semi-enclosed brackish system

Gustaf Dalen AERONET site, an examplar of lighthouse design

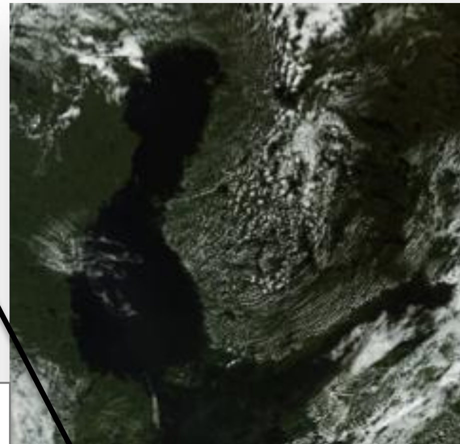

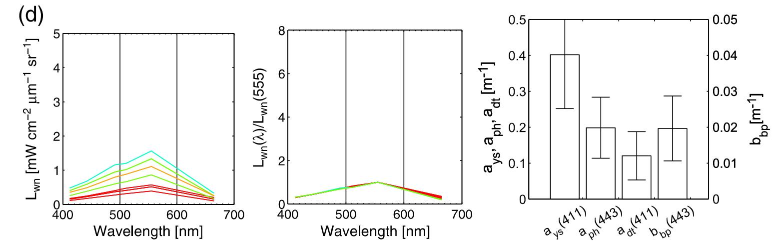

Fig. 4. Sample cases identified in Fig. 2 through letters a–d for different areas of the feature map obtained from the first two PCA components. The first column displays non-normalized L_{WN} spectra, the second column displays the former spectra normalized with respect to $L_{WN}(555)$, the third column illustrates the related absorption (a_{ys}, a_{ph} and a_{dt}) and backscattering (b_{bp}) components with the error bar indicating ±1 standard deviation.

Spectral and PCA analyses for high gelbstoff Baltic waters. Zibordi et al 2011

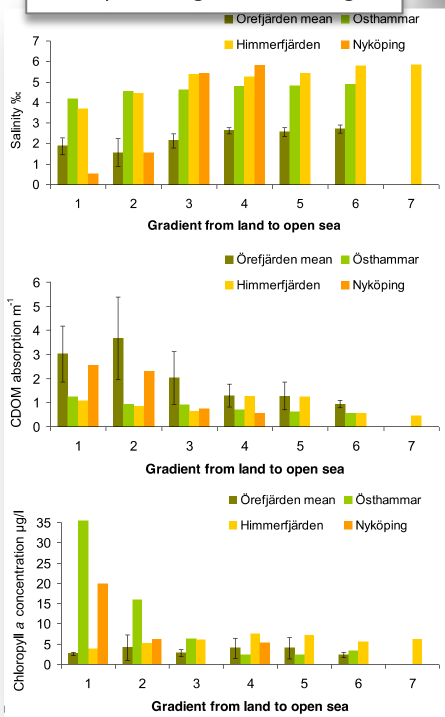

Bio-optical gradients in the Gulf of Bothnia and Central Baltic. Harvey et al 2012, Coastcolour UCM.

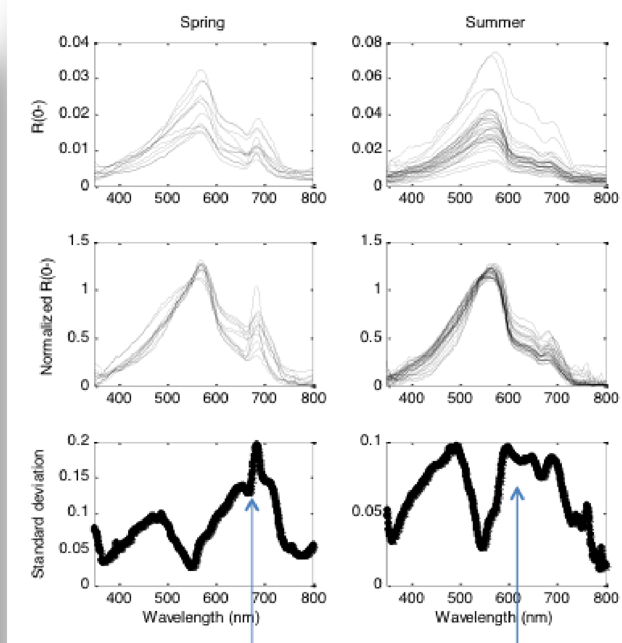

Two contrasting phytoplankton populations shape the reflectance spectrum in the Baltic. Eukaryotic chl-a and sun-induced fluorescence dominate in spring, whilst prokaryotic phycobilipigments and chl-a dominate in summer. Simis et al.,in prep

The North Sea: a tidally-dominated system with dynamically variable Case 2 influence

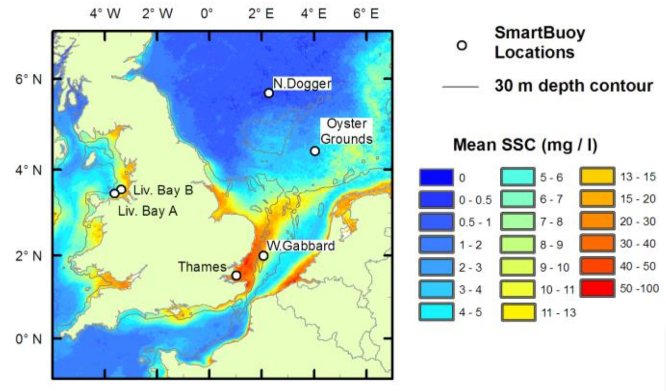

Figure 3.2: SmartBuoy locations. The SPM background is the MODIS January monthly mean map.

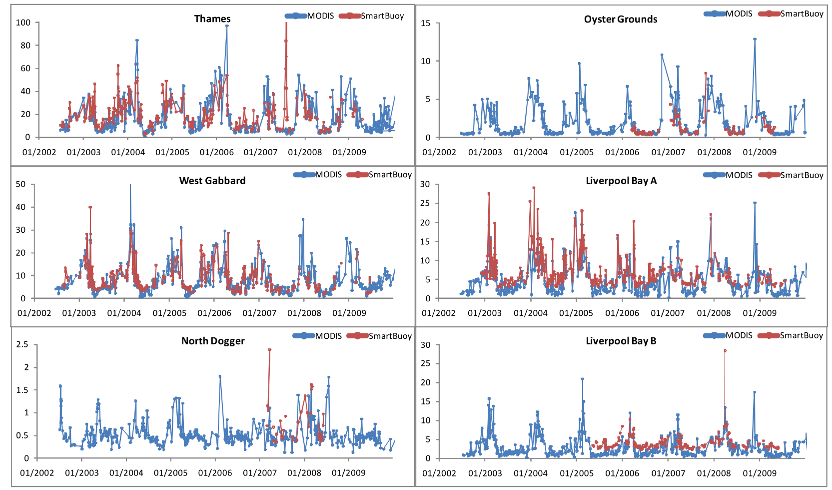

Variability in SmartBuoy/MODIS derived SPM concentrations. Dolphin et al 2011

Figure 4.2: Time series of MODIS satellite derived SPM measurements for six SmartBuoy locations, with matching SmartBuoy in situ measurements.

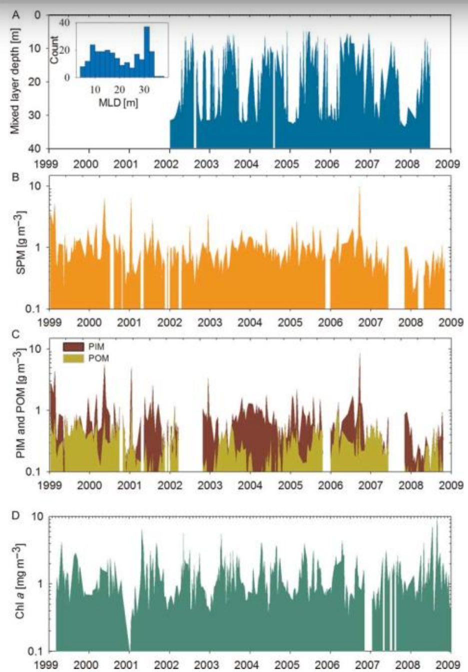

Fig. 1. Weekly time series at L4 between January 1999 and January 2009: (**A**) mixed layer depth (insert is histogram of frequency), (**B**) suspended particulate matter concentration, SPM, (**C**) inorganic and organic particulate matter concentration (PIM and POM), (**D**) Chlorophyll *a* concentration, Chl *a*. Broken line corresponds to missing data.

Inter-annual, seasonal and higher frequency variability in the western English Channel. Martinez-Vicente et al, 2010.

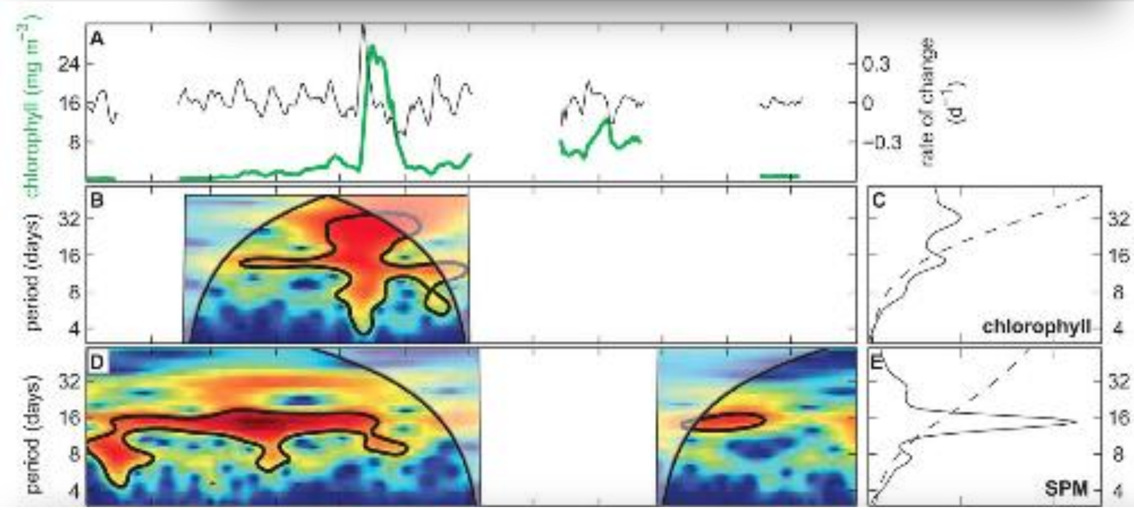

Figure 6. Wavelet analysis of chlorophyll, SPM, salinity and temperature on a daily time scale. (A) Original time series (green line) and transformed time series (rate of change, black line) of daily averaged chlorophyll concentration in the year 2007. (B-I) Wavelet power spectra (left panels) and global wavelet spectra (right panels) of daily averaged data of (B, C) chlorophyll concentration, (D, E) SPM concentration, (F, G) salinity, and (H, I) temperature. The wavelet power spectra show only the year 2007; the global wavelet spectra are based on the complete time series (2001–2009). See the legend of Fig. 3 for an explanation of wavelet power spectra.
doi:10.1

Wavelet analyses of the WARP SMartBuoy, showing the very strong influence of the tidal cycle, from ± 6hrs semidiurnal to 15 day spring/neap cycle. Blauw et al 2012.

The North Sea: a tidally-dominated system with dynamically variable Case 2 influence

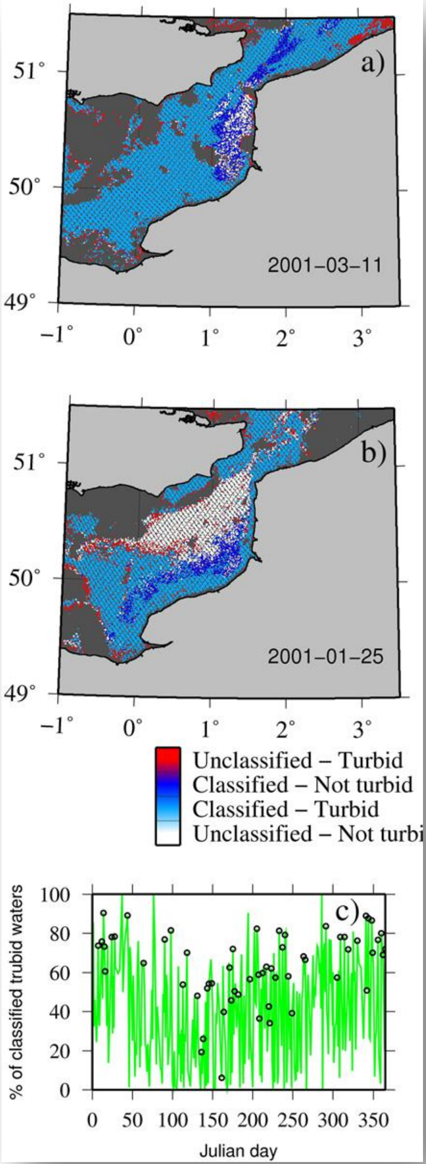

Dominance of turbid waters in the eastern English Channel . Vantrepotte et al, 2012.

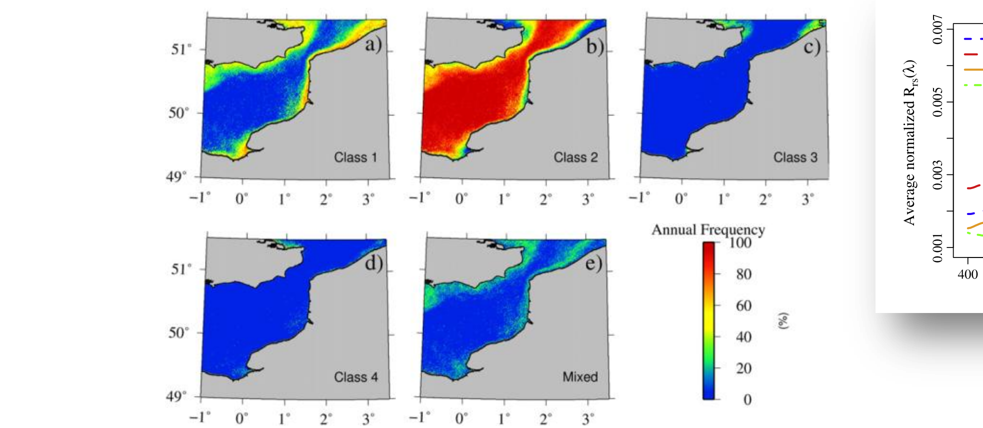

Fig. 6. Annual membership frequency (in %) associated with the 4 reference optical classes (a, b, c, d) and optically mixed (d) spatial distribution obtained from SeaWiFS daily data in 2001 in the eastern English Channel and Southern North Sea.

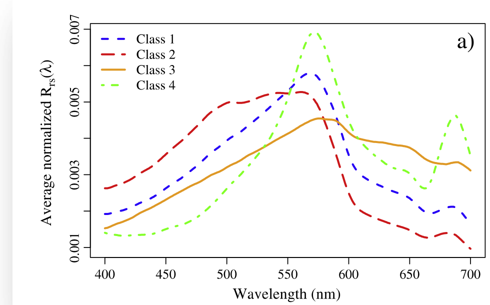

Persistence of various classes Case 2 waters in the English Channel & southern North Sea. Vantrepotte et al, 2012.

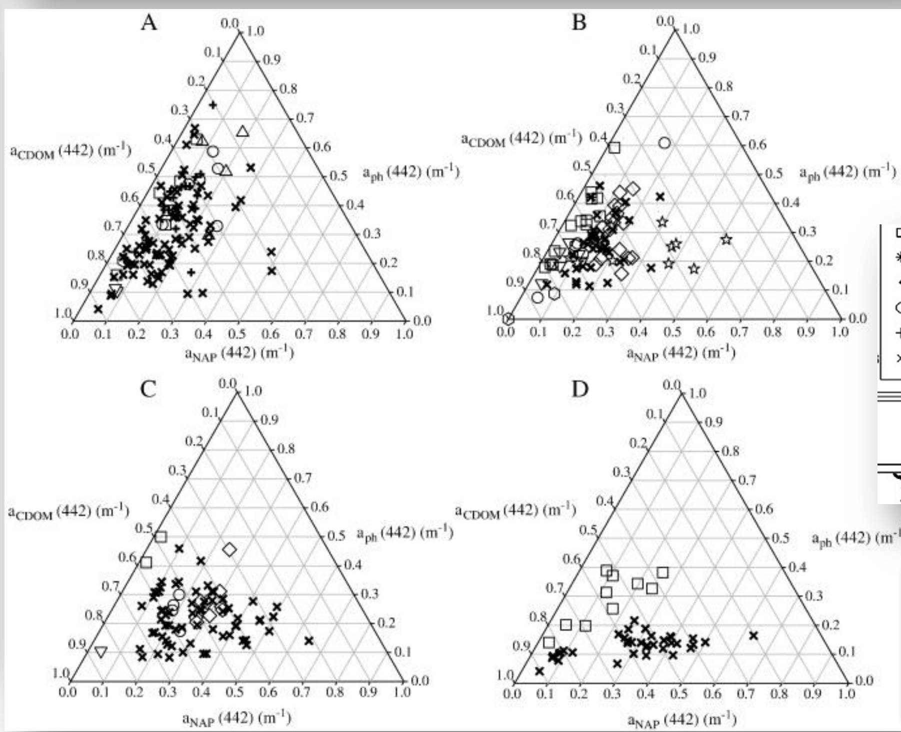

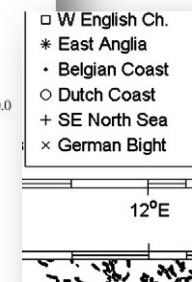

Ternary plots showing regional variability of Case 2 influences across the North Sea and English Channel. Tilstone et al 2012

Lake Erie: a shallow eutrophic dominated by wind and riverine variability

Microcystis bloom in Lake Erie, September 2011, from MERIS FR data . ESA

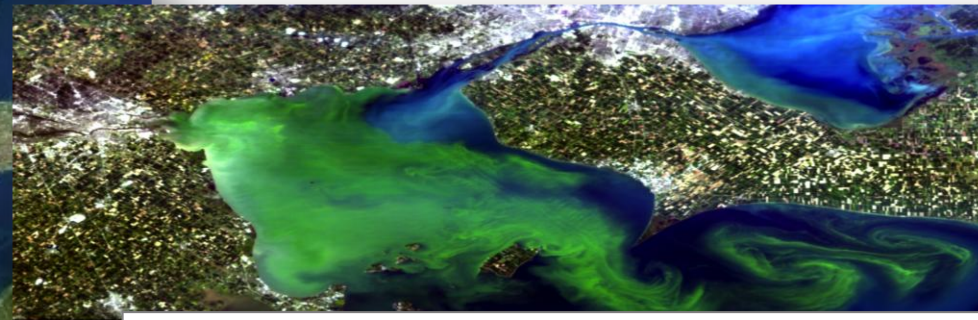

Microcystis bloom in Lake Erie, September 2011, HICO

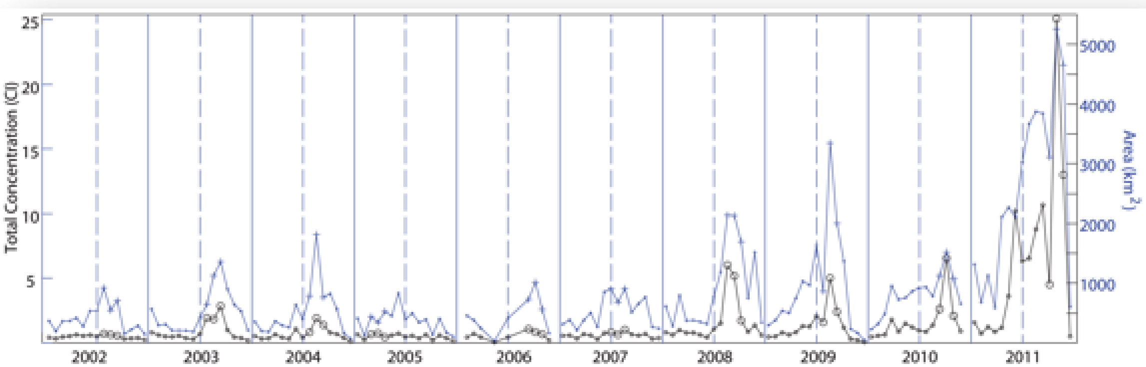

Time series of bloom intensity (black) and area >0.001 CI (blue) from the cumulative CI for each 10-day composites. Stumpf et al 2012.

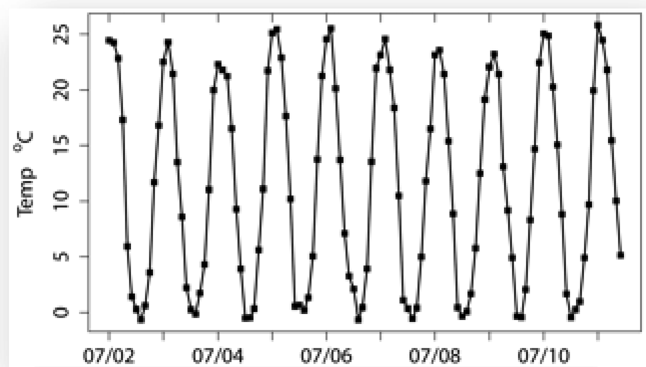

Monthly mean water temperature in western Lake Erie from 2002–2011. Stumpf et al 2012.

Hartbeespoort Dam: a small hypertrophic water body with a significant *Microcystis* problem…

Pseudo true-colour image Hartbeespoort Dam ± 4 x 10 km, SumbandilaSat, May 2010. Meyer, unpublished

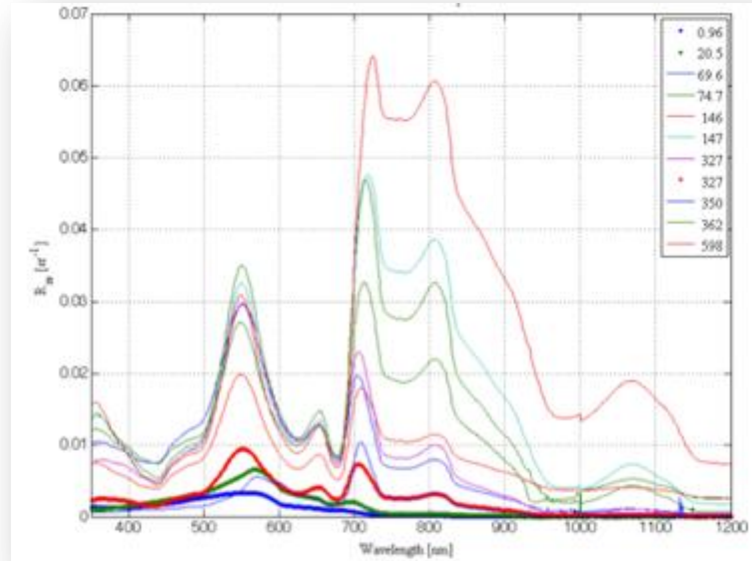

Sample above-water R_{rs} spectra from Zeekovlei, Loskop and Hartbeespoort Dams. Matthews, unpublished

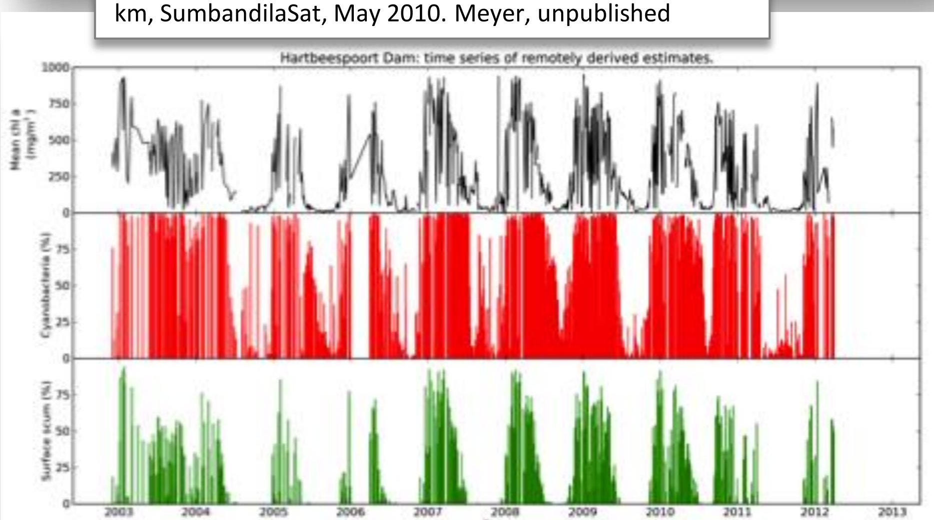

10 year time series of phytoplankton biomass (top), percentage cyanobacteria (middle), and percentage surface scums (bottom) for Hartbeespoort Dam, using the MPH algorithm applied to MERIS FR data. Matthews IOCCG/GEOHAB in prep

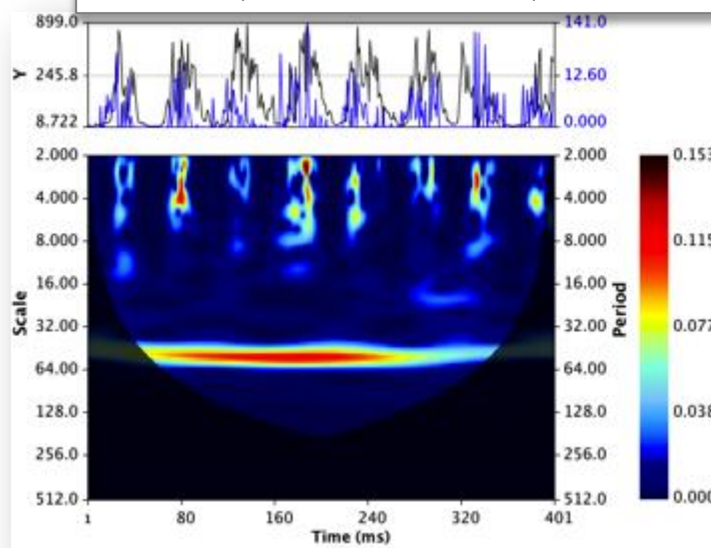

X-wavelet analysis of phytoplankton biomass vs precipitation for the same Hartbeespoort time. Pienaar et al in prep

Preliminary summary: ocean colour requirements for diverse coastal and inland waters

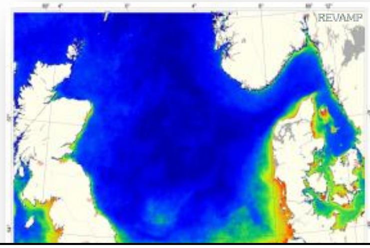

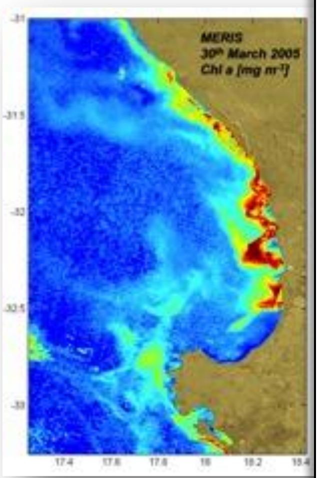

- "Operational" has some diversity of meaning, but coastal and inland waters users require rapid, routine access to operational high quality application-focused products

- What are the user needs? A wide range, but include water quality & eutrophication indices; phytoplankton, sediment and biogeochemical dynamics; harmful algal bloom/PFT indicators for both real-time operational and long term ecosystem characterisation…..

- What is the primary event scale and how important is it to resolve? Dynamic wind driven systems, such as the Benguela and Baltic, need a *resolved* observation frequency of < 3 days for phytoplankton ecology applications. Tidally and eutrophic inland systems need a < weekly resolved observation frequency, although this does not address the highest frequency events….

- What range of optical complexity must be addressed? All systems need the ability to resolve large intra-image variability e.g. oligotrophic to hypertrophic, mesotrophic to Case-2 sediment or gelbstoff dominated waters…..

- Very strong case for geostationary sensors…..

Challenges of using Ocean Colour Radiometry for HAB detection

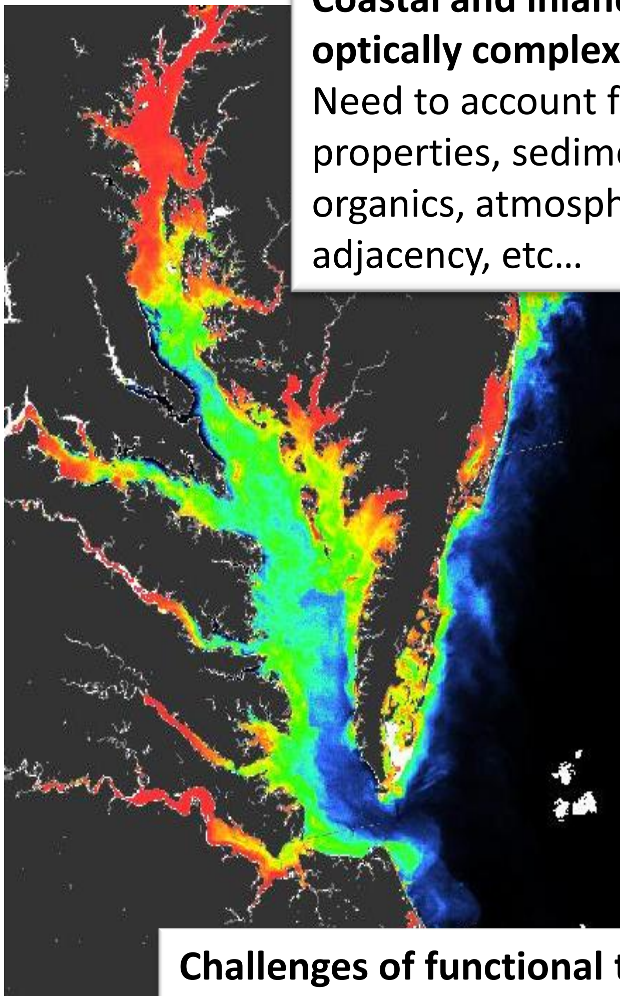

Coastal and inland waters optically complex & dynamic
Need to account for algal properties, sediments dissolved organics, atmosphere, land adjacency, etc…

Challenges of functional type detection
What information can realistically be provided on assemblage structure in coastal/inland waters?

Stratification of blooms & motility
Example: migrating high biomass (>500 mg m^{-3}) dinoflagellate blooms in Monterey bay

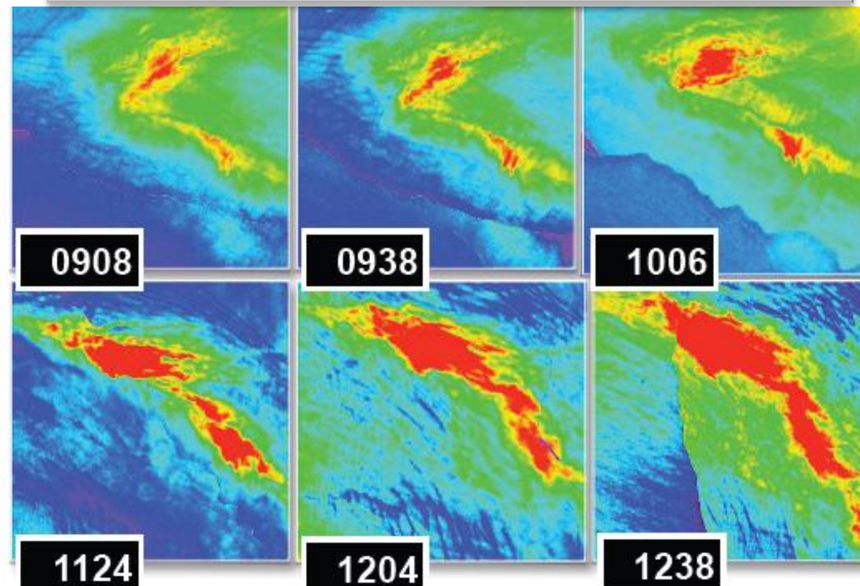

Courtesy Raphe Kudela

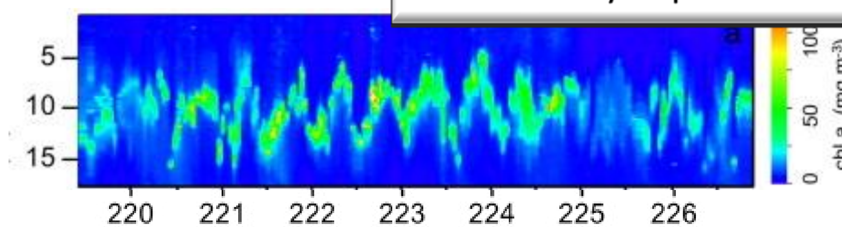

Many HABs harmful at low biomass
A. tamarense toxic at only 10^3 cells l^{-1}

IOCCG/GEOHAB WG HABs & Ocean Colour, in prep

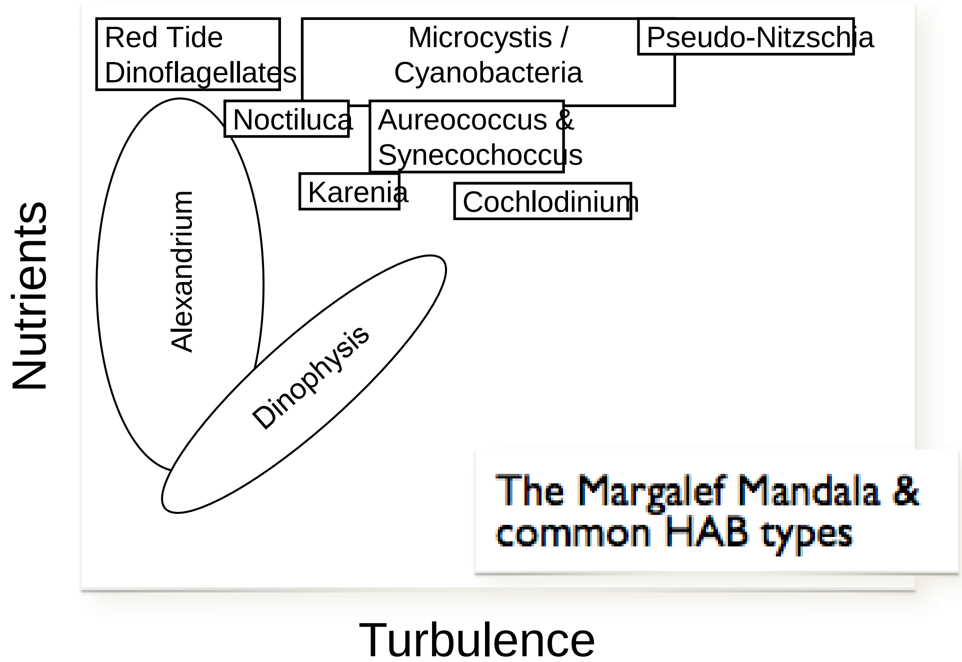

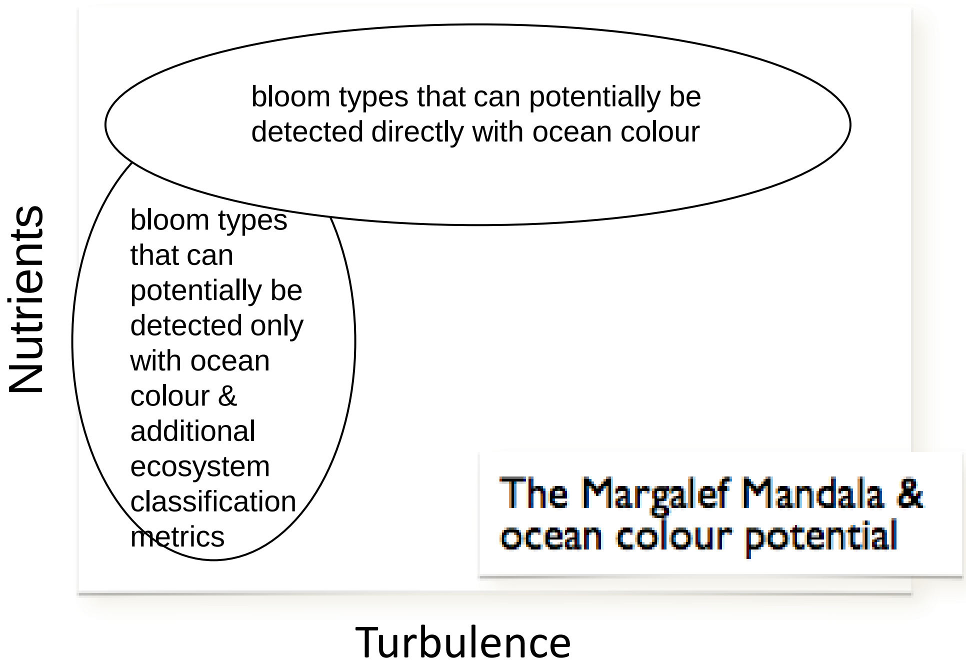

The Ecosystem Perspective

The Margalef mandala is a common way of examining algal succession by characterising the ecological niche in which different species or groups are most likely to proliferate.

Many harmful algal species can have impact at very low cell concentrations, as a minor component of the algal assemblage, or as subsurface blooms with no bio-optical surface expression.

Viewing the mandala from an ocean colour perspective, it is clear that only high nutrient-demand/biomass blooms are likely to be *directly* detectable using ocean colour - regardless of the algorithm type or technique used.

Using ocean colour as one component of a multi-parameter ecosystem classification - effectively using the mandala to create an earth observation based metric - will potentially allow the detection of some other bloom types.

IOCCG/GEOHAB WG HABs & Ocean Colour, in prep

Spectral characterisation and causality analyses for Case 2 waters

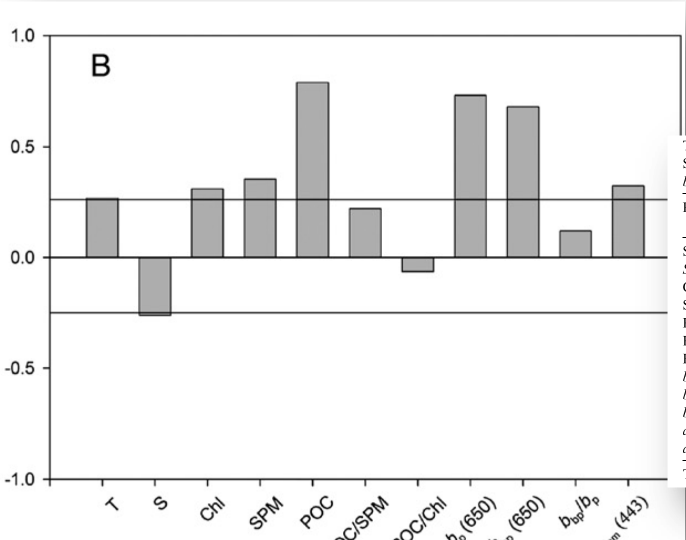

Table 2
Statistical parameters of SST, S, Chl, SPM, POC, POC/SPM, POC/Chl, b_p, b_{bp}, b_{bp}/b_p, a_{cdom}, and $a_p/(a_p+a_{cdom})$, calculated over the whole studied area

Parameters	Mean	Standard deviation	Coefficient variation (%)	Minimum	Maximum
SST	11.7	2.9	24	7.3	16.7
S	33.9	1.5	4	23.1	35.4
Chl	8.3	6.9	83	0.7	33.2
SPM	14.7	12.2	83	3.2	87.4
POC	0.75	0.39	51	0.21	2.89
POC/SPM	0.067	0.044	66	0.008	0.445
POC/CHL	154	135	88	30	690
b_p (650)	1.44	1.04	70	0.29	6.45
b_{bp} (650)	0.020	0.023	115	0.002	0.109
b_{bp}/b_p	0.013	0.008	61	0.003	0.036
a_{cdom} (443)	0.15	0.12	80	0.01	0.64
$a_p/(a_p+a_{cdom})$	0.74	0.15	20	0.37	0.97

The coefficient of variation is the standard deviation divided by the mean.

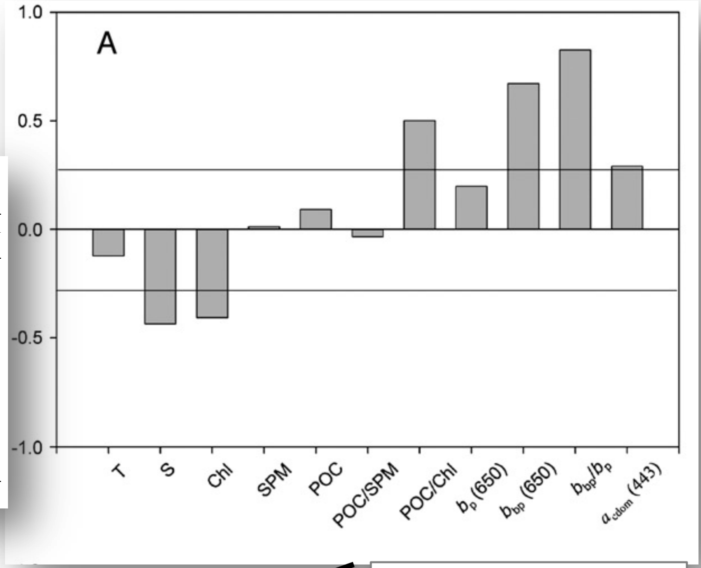

First EOF mode (74%): strong correlation with backscattering, backscattering probability and POC/Chl ratio, indicating effects of concentration & nature of suspended material . Lubac & Loisl 2007.

Second EOF (15%) dominated by absorption and fluorescence processes. Lubac & Loisl 2007.

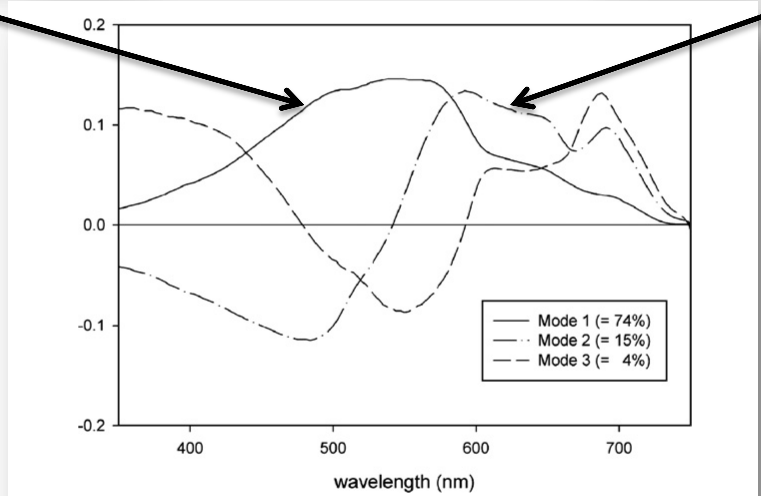

Fig. 5. The first three dominant empirical orthogonal function (EOF) mode spectra explain 93% of the total $R_{rs}(\lambda)$ variance. EOF mode 1 (solid curve) accounts for 74% of the total R_{rs} variance, EOF mode 2 (dash–dot curve) accounts for 15% of the total R_{rs} variance, and EOF mode 3 (dash curve) accounts for 4% of the total R_{rs} variance.

Spectral characterisation of reflectance data with increasing phytoplankton biomass

±150 remotely sensed reflectance spectra from TSRB & ASD with corresponding fluorometric/photometric Chl a data, from the southern Benguela, Zeekoevlei (hypertrophic), Hartbeespoort (hypertrophic), Loskop (oligo-hypertrophic)

Principal Component Analysis and 2[nd] order derivative (Savitsky-Golay)

Chl *a* < 3 mg m^{-3}	3 < Chl *a* < 15 mg m^{-3}	Chl *a* > 15 mg m^{-3}

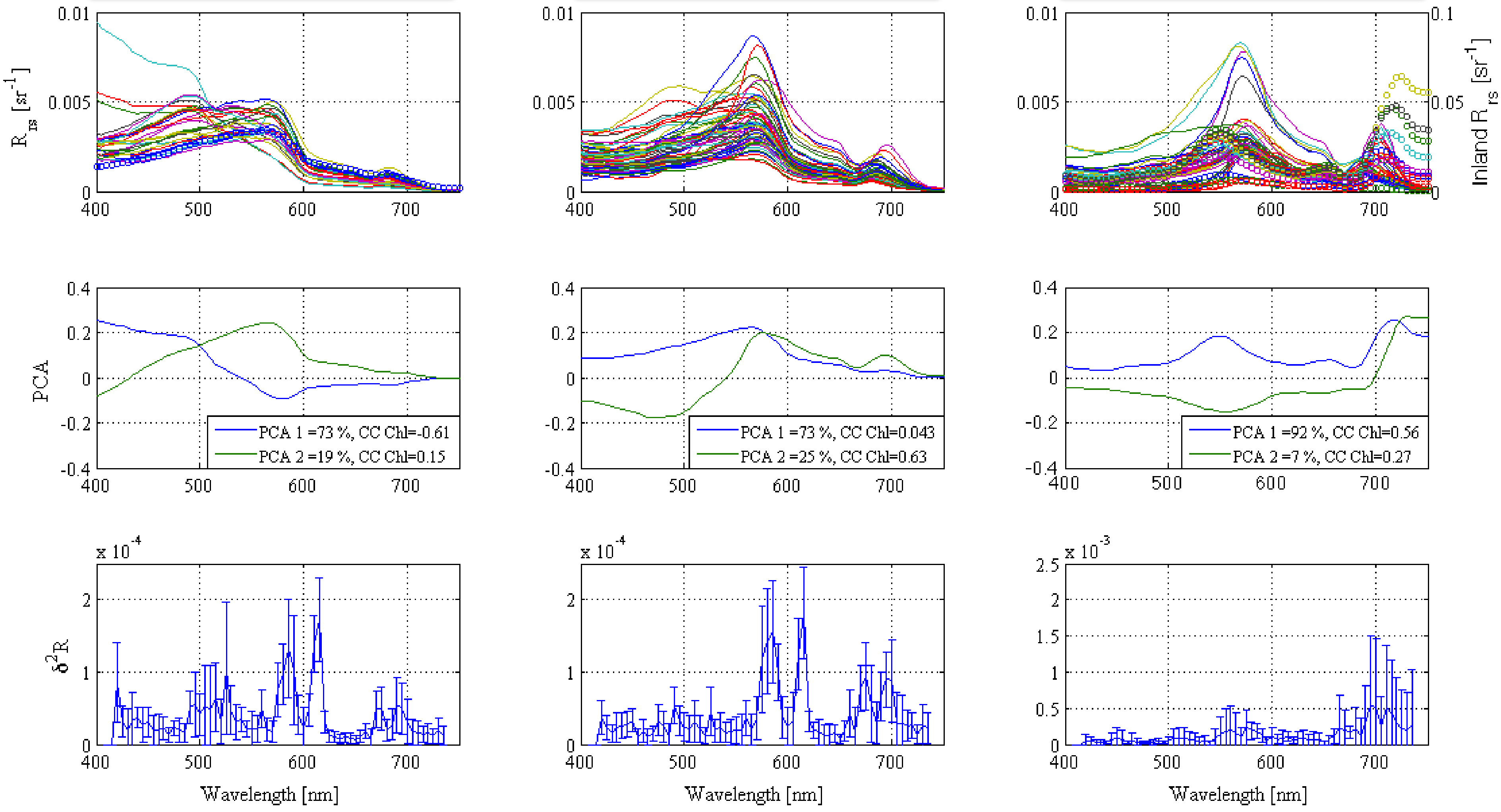

Characterisation of marine eukaryote associated reflectance data at high biomass

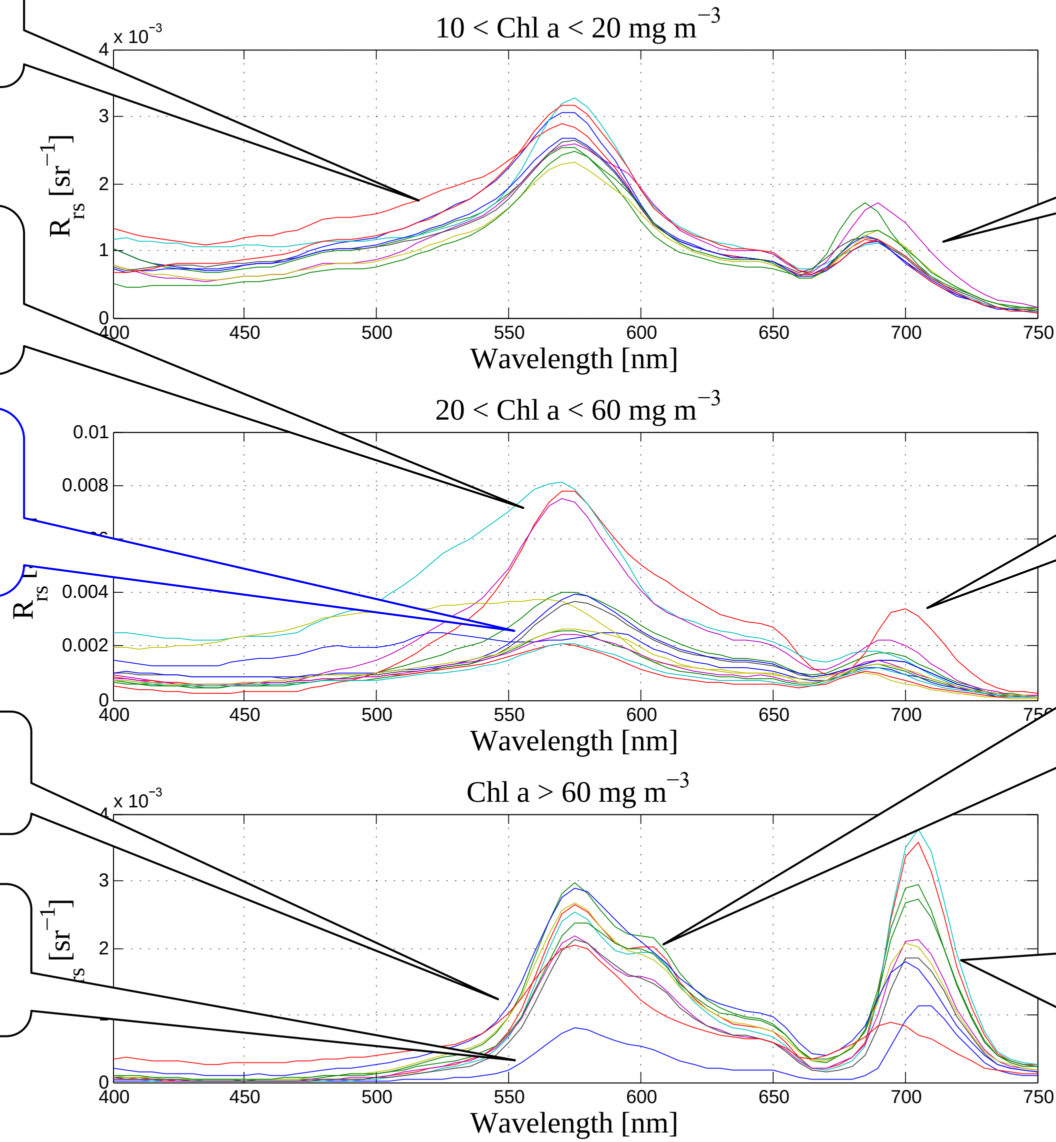

Majority diatom dominated

Dinoflagellate/coccolithophore dominated

M. rubrum dominated with phycoerythrin absorption

Dinoflagellate dominated

Alexandrium catenella bloom Chl a = 310 mg m^{-3}

Signal in red primarily fluorescence with quantum yields of < 0.5%

Some shift towards 709 nm as absorption/backscattering processes seen in combination with fluorescence

Inflection point appears related to secondary chl a/c absorption peaks ± 620nm in both a & bb

Signal in red primarily at 709 nm peak as absorption/backscattering dominates

Characterisation of inland prokaryote/eukaryote reflectance data at high biomass

Sample remotely sensed reflectance spectra acquired with above-water ASD from Zeekoevlei (hypertrophic), Hartbeespoort (hypertrophic), Loskop (oligo-hypertrophic)

Typical TSS values of 0.1 to 300 mg l^{-1}, of which phytoplankton contribute 20% to 100%

Eukaryote assemblages (•) dominated by mixed or *Ceratium* species

Prokaryote assemblages (-) dominated by *Microcystis* species

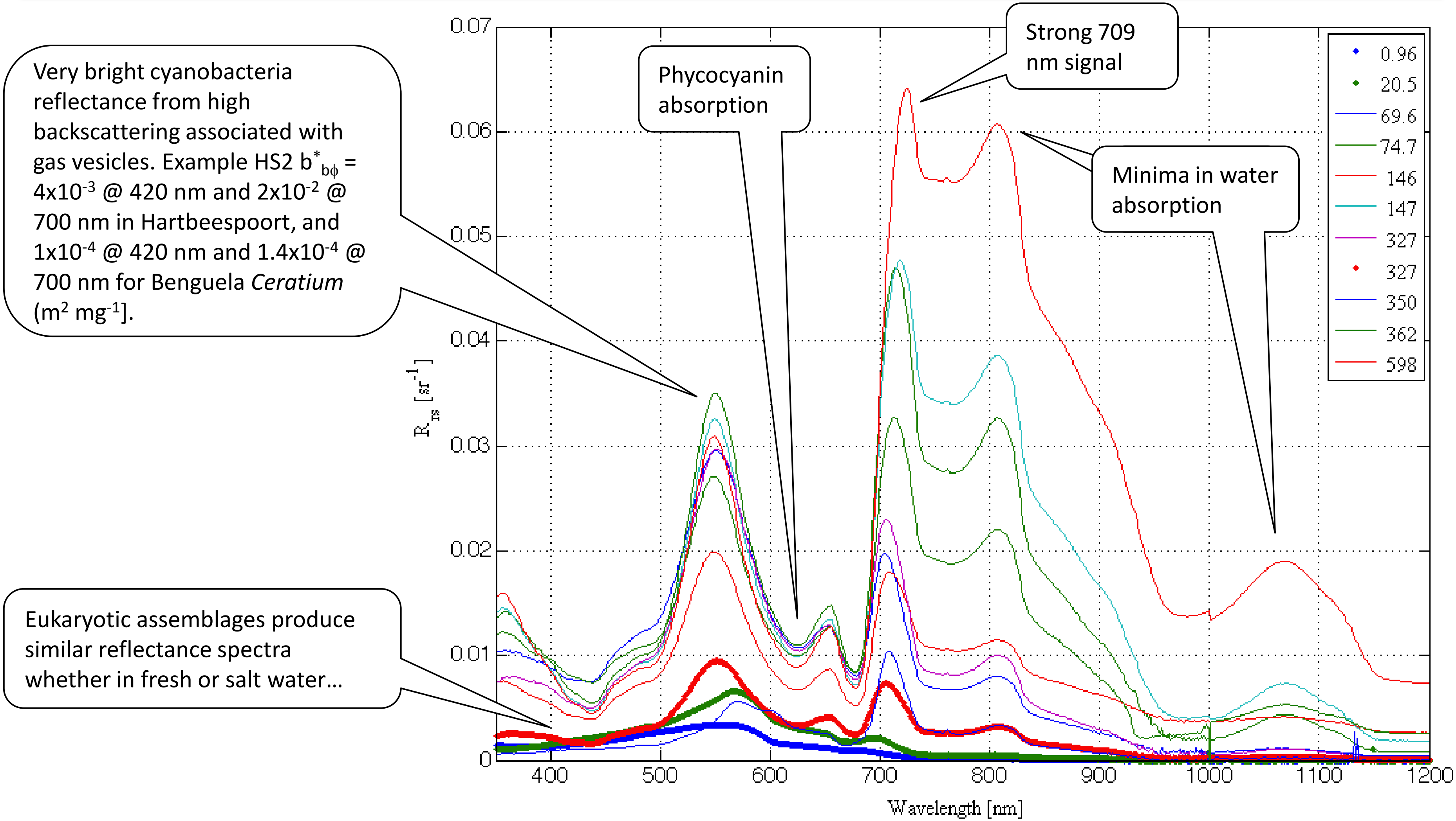

Coupled radiative transfer models: better understanding constituent contributions to the ocean colour signal

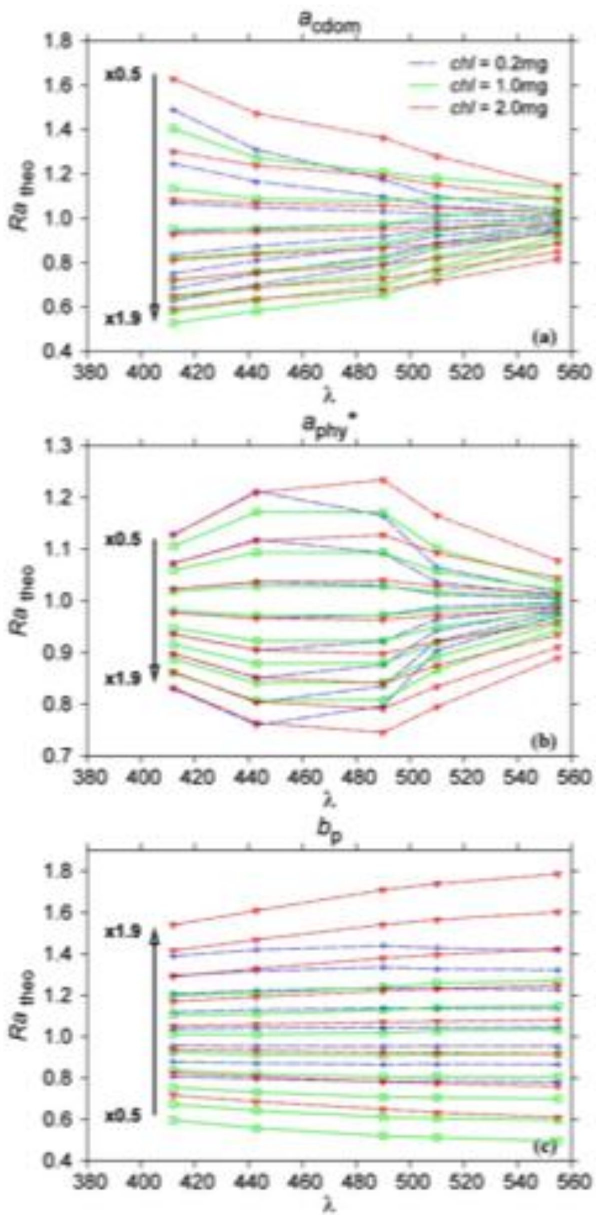

Understanding systematic variations in ocean colour radiance needs a combination of modelling & empiricism. This combined approach is the only way to fully understand causality with regard to resolving first order effects of biomass and constituent change in complex waters and second order phytoplankton functional type variability & effect.

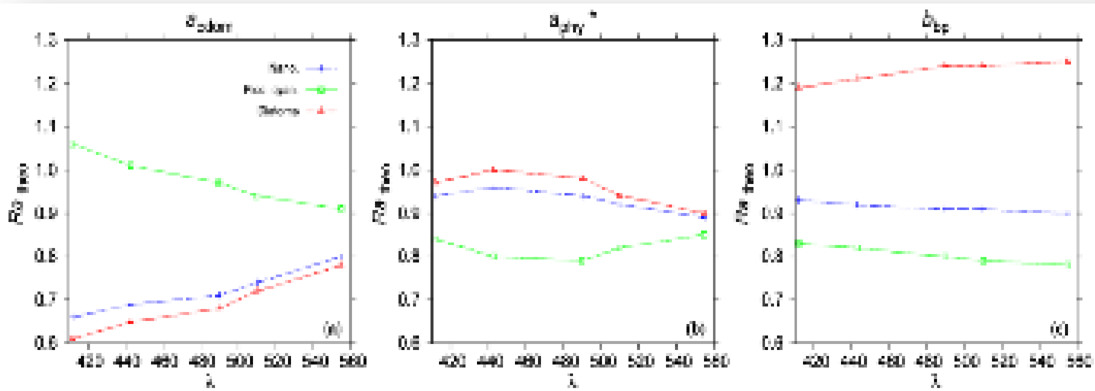

Fig. 6. Theoretical mean radiance anomalies as a function of wavelength, in response to variation in a_{cdom} (a), a^*_{phy}(b) and b_p(c) for a chlorophyll a concentration of $1 mg.m^{-3}$. Results are obtained for realistic parameters variations for the following phytoplankton groups: nanoeucaryotes (blue), picoplankton cyanobacteria (green) and diatoms (red).

Preliminary signal analysis of PHYSAT based on bio-optical environment. Alvain et al., 2012

Modelling systematic variability in phytoplankton IOPs and effects on the light field: Equivalent algal population coupled IOP/radiative transfer model

Eukaryote:
core = cytoplasm
shell - chloroplast

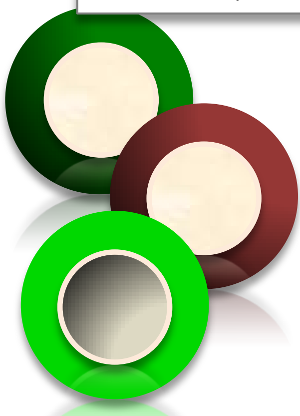

Prokaryote:
core = gas vacuole
shell - chromatoplasm

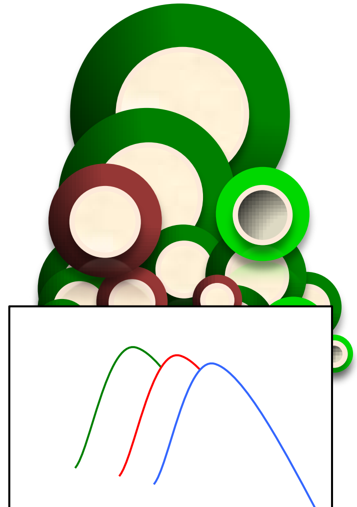

Phytoplankton functional type distributions

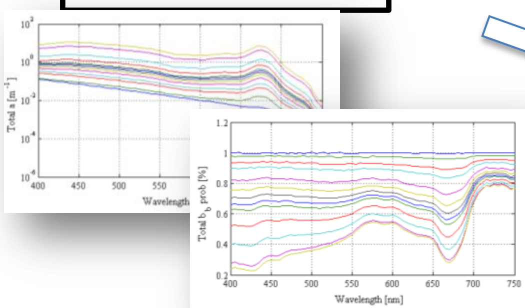

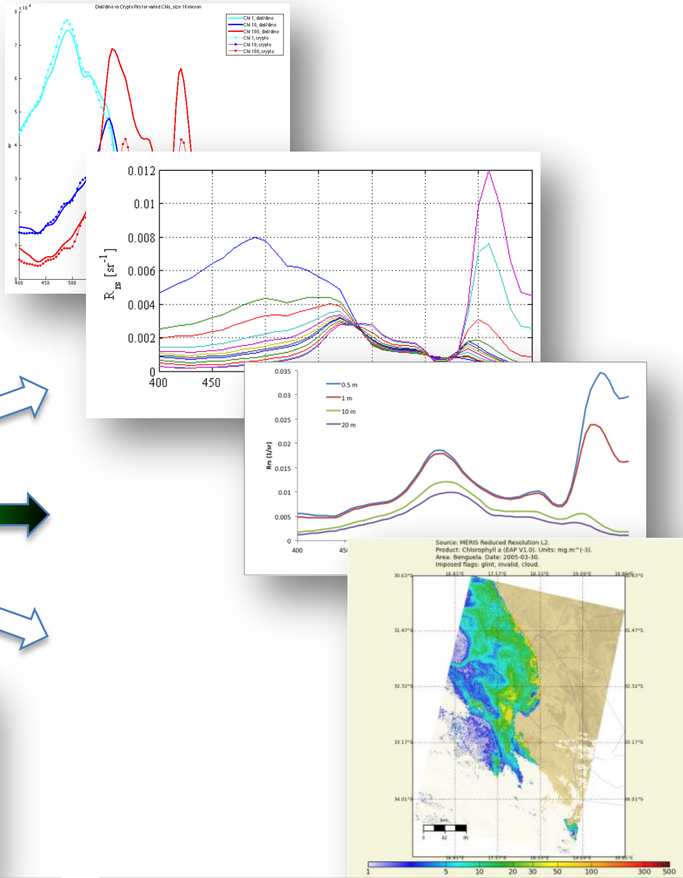

Two layered sphere model allows IOP modelling of various eukaryotic (Bernard et al 2009) and vacuole containing prokaryotic (Matthews et al submitted) functional types. Allows for variations in size, ultrastructure, pigment complement & density,….

Equivalent algal population models allows creation of admixtures of functional types based on effective diameter & diversity manipulated particle size distributions. Bernard et al 2007, 2009, Robertson et al in prep

Equivalent algal population IOPS, including phase functions, coupled to Hydrolight, Ecolight and Ecolight-S radiative transfer models for forward and inverse applications. Robinson et al in prep

Modelling systematic variability in phytoplankton IOPs and effects on the aquatic light field

- All phytoplankton IOPs from 16 μm effective diameter two-layered “dino/diatom” population model
- Non-linear scaling with Chl a of gelbstoff/detrital absorption and non-algal backscattering using simple spectral slope models
- Spectrally variant Fournier-Forand phase functions based on total backscattering probability
- Fluorescence quantum yield varying from 0.8% to 0.2% with Chl a concentration

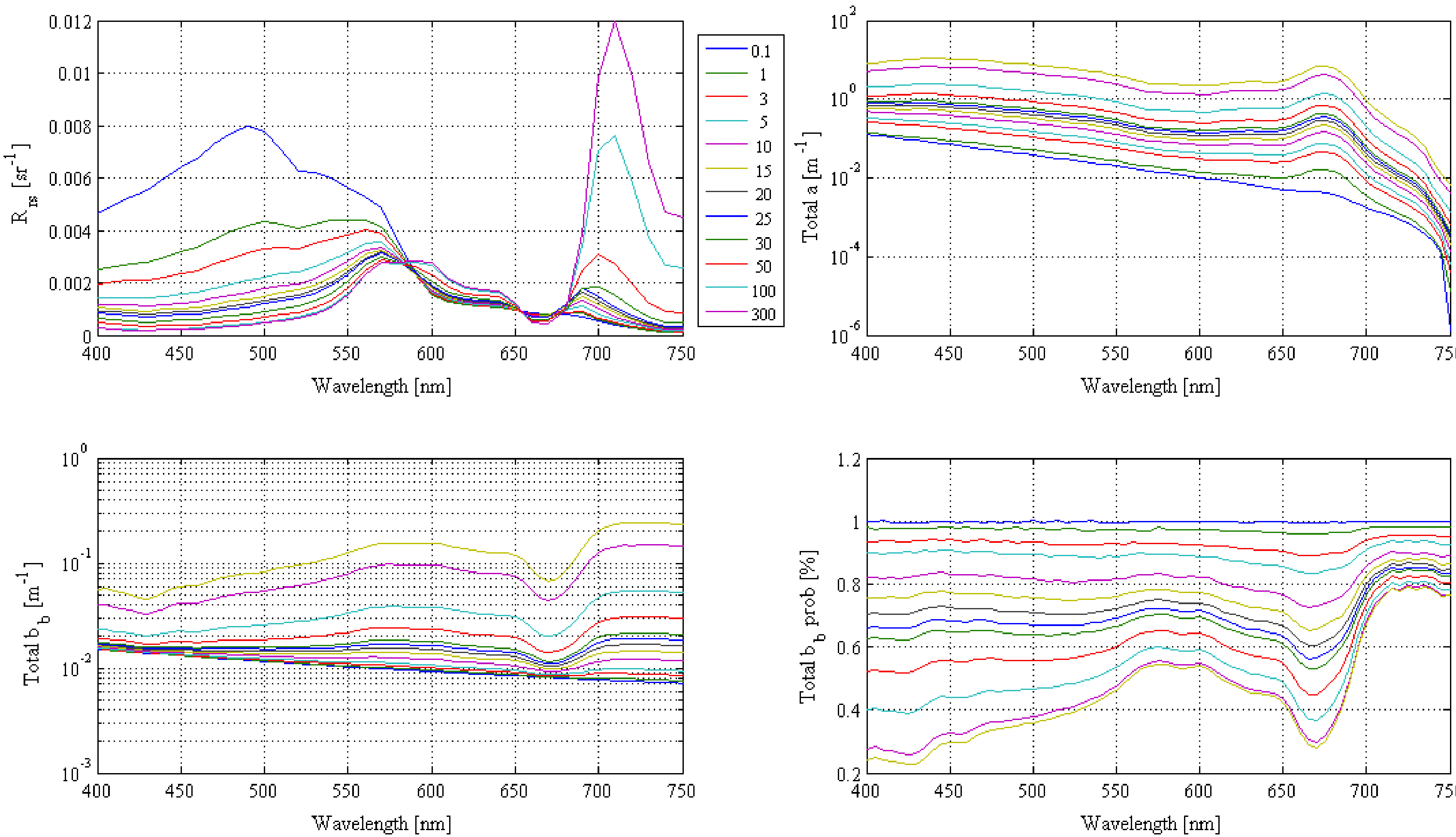

Coupled radiative transfer models: effects of phytoplankton size at changing biomass

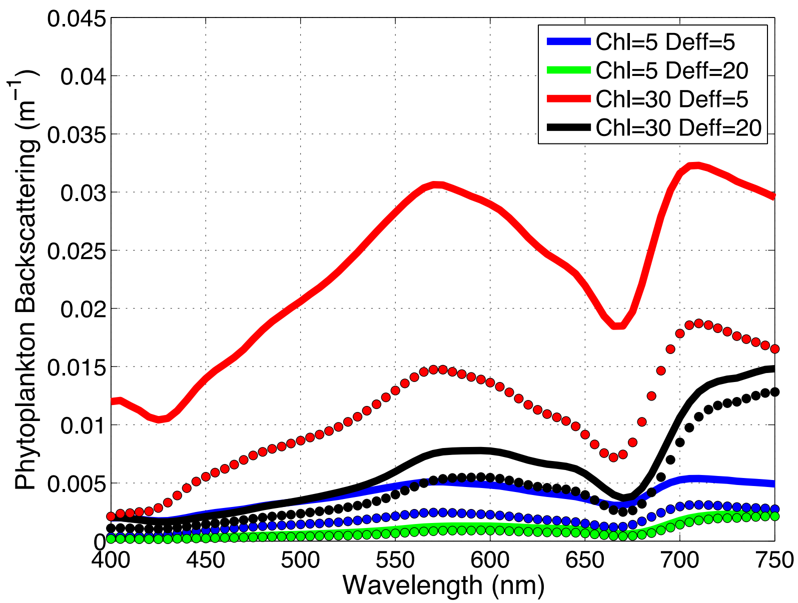

Example demonstrating the potential effects on ocean colour of varying assemblage size, as given by the effective diameter of the population, with different parameterisations of ci (the chlorophyll a density per cell)as one of the key phytoplankton IOP variables

Static ci = 2.5 kg m-3 (lines)
Variable ci as below (dots)

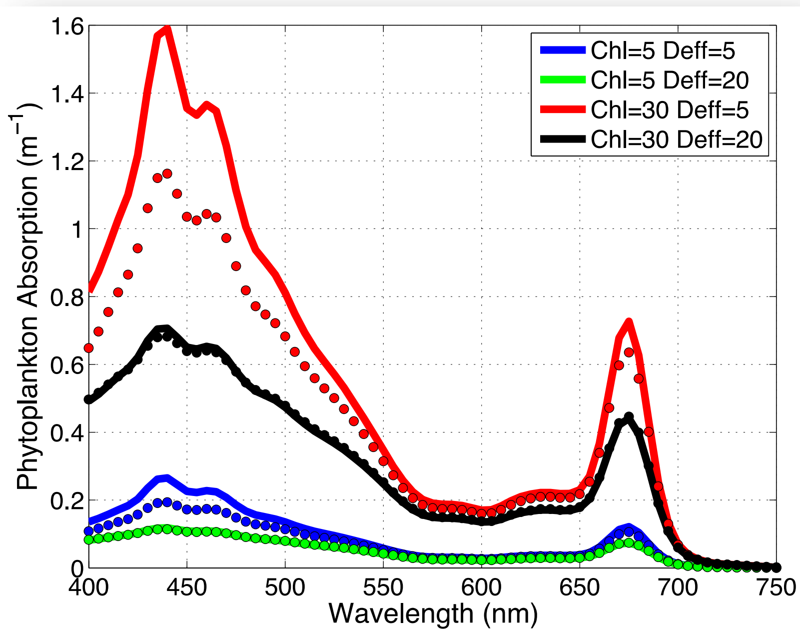

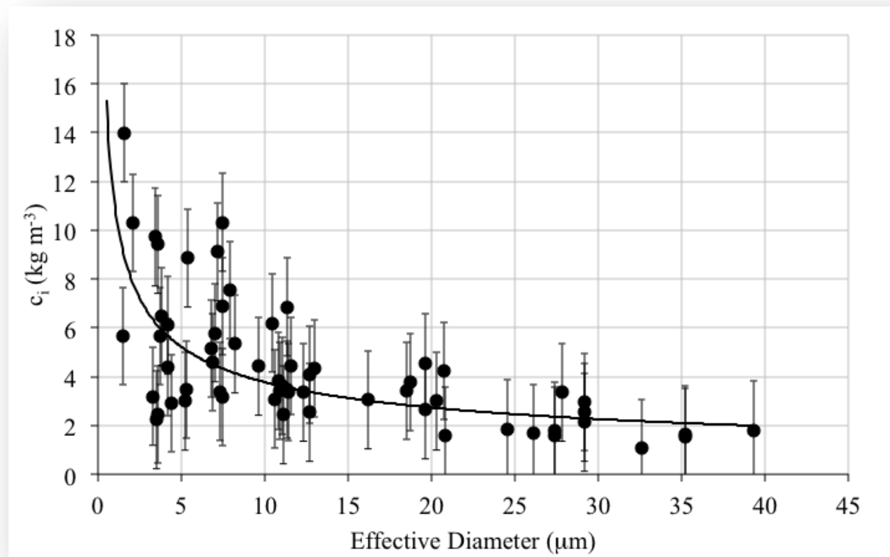

Coupled radiative transfer models: effects of phytoplankton size at changing biomass

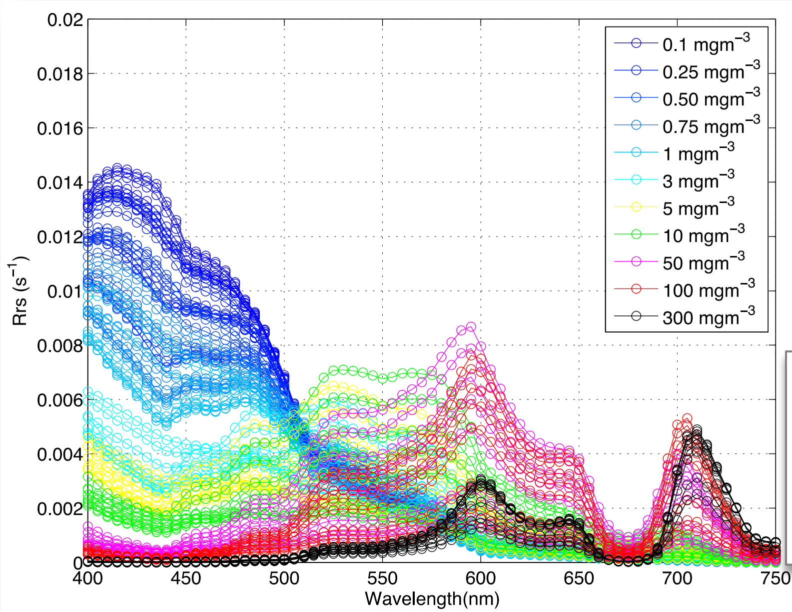

Ranges of effective diameters from 2 to 50 μm across chl range

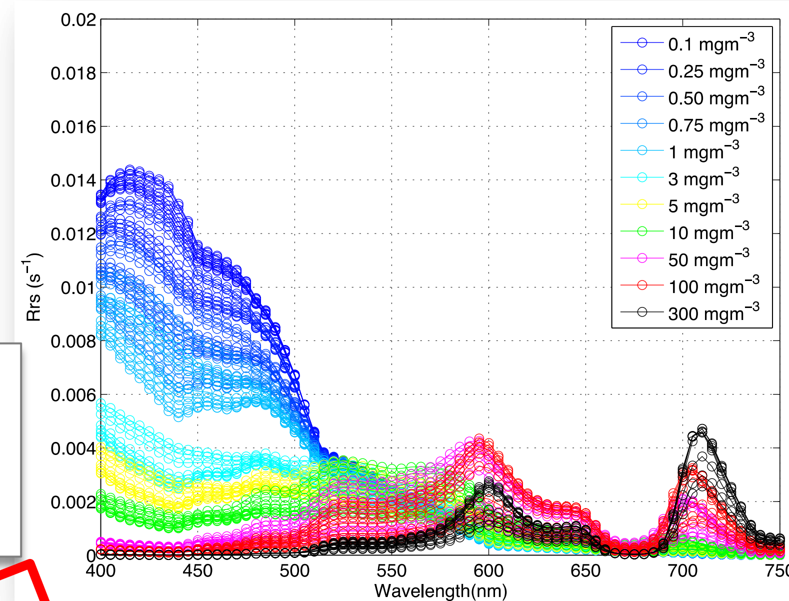

Static c_i

Dynamic c_i

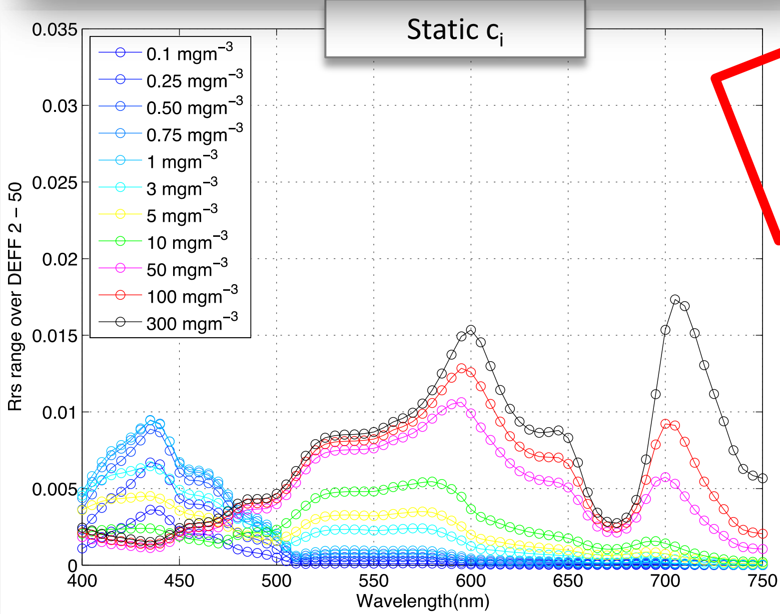

No allometric abundance law or diversity represented here so caveat emptor

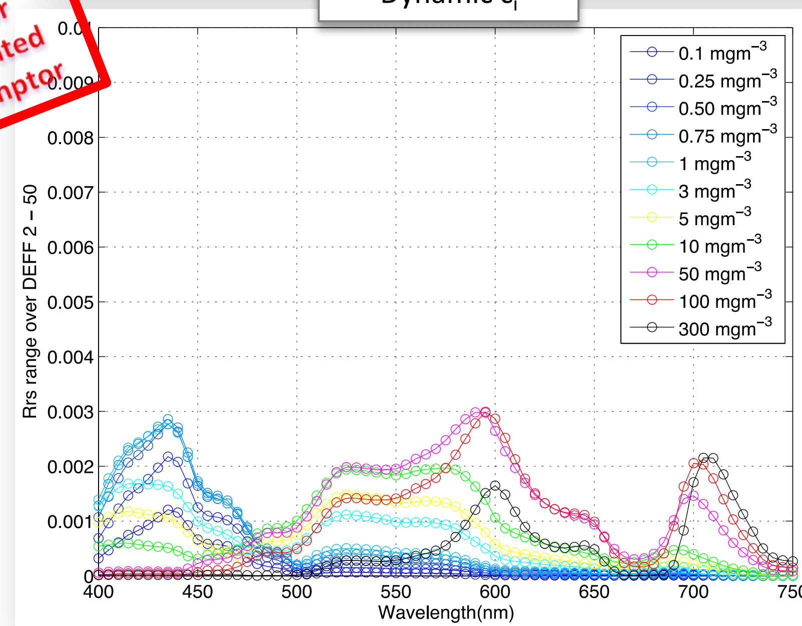

Coupled radiative transfer models: effects of phytoplankton pigment variability at changing biomass

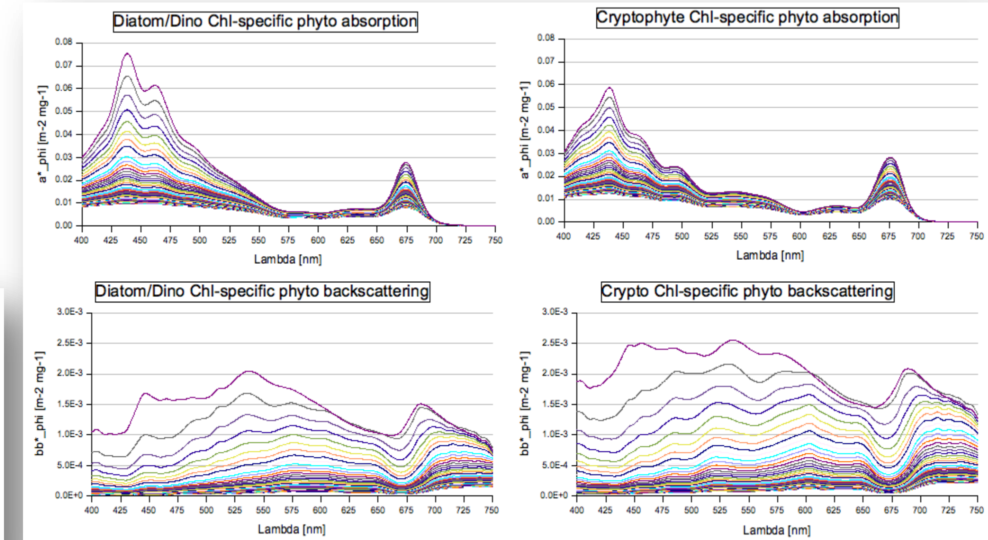

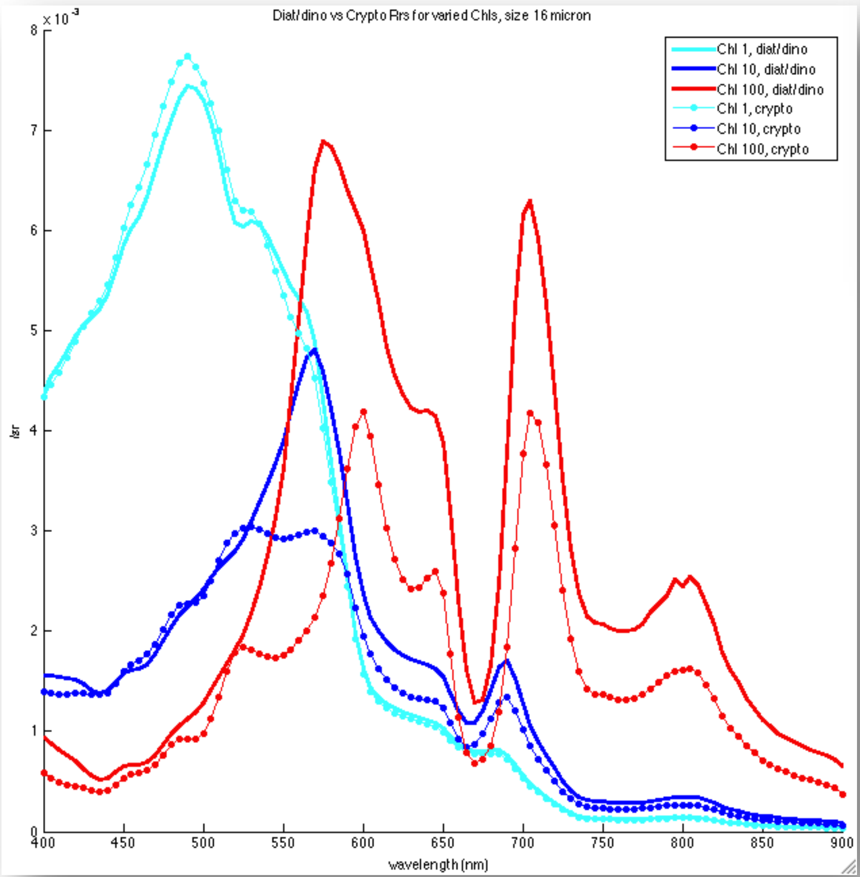

Example demonstrating the potential effects on ocean colour of varying pigment based functional types, as given by the IOP basis vectors for a dinoflagellate/diatom assemblage and a crytophyte-based assemblage (here approximately representing the autotrophic ciliate *Mesodinium rubrum*)

Coupled radiative transfer models: better understanding constituent contributions to the ocean colour signal

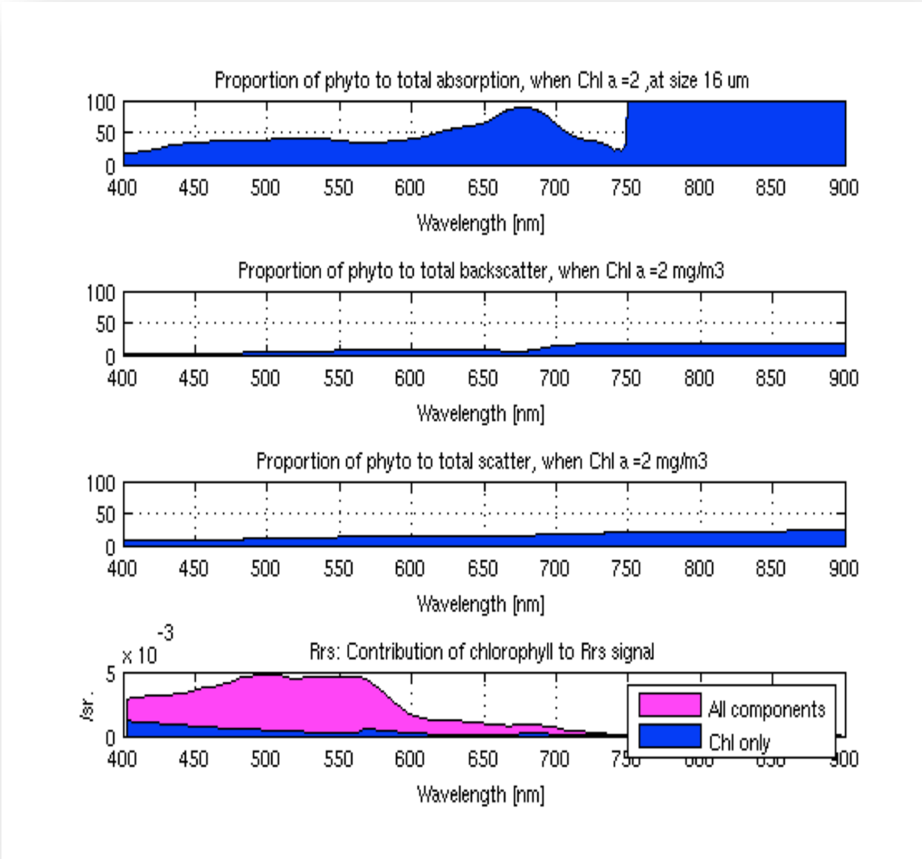

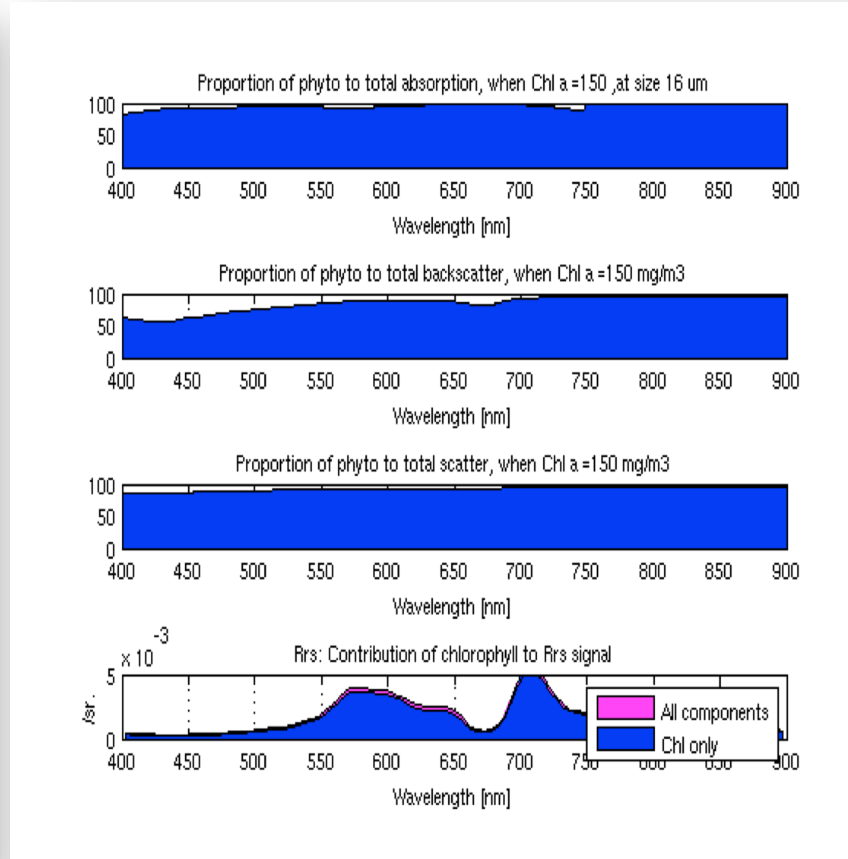

Relative contribution of phytoplankton to the water leaving signal at 2 mg m^{-3} and 150 mg m^{-3}.

Coupled radiative transfer models: effects of gas vacuoles on IOPs

Increasing gas vacuole volume causes increased backscatter & decreased forward scattering

Model reproduces to first order observed features for gas vacuolate cells in the attenuation and Volume Scattering Function

Matthews et al in prep

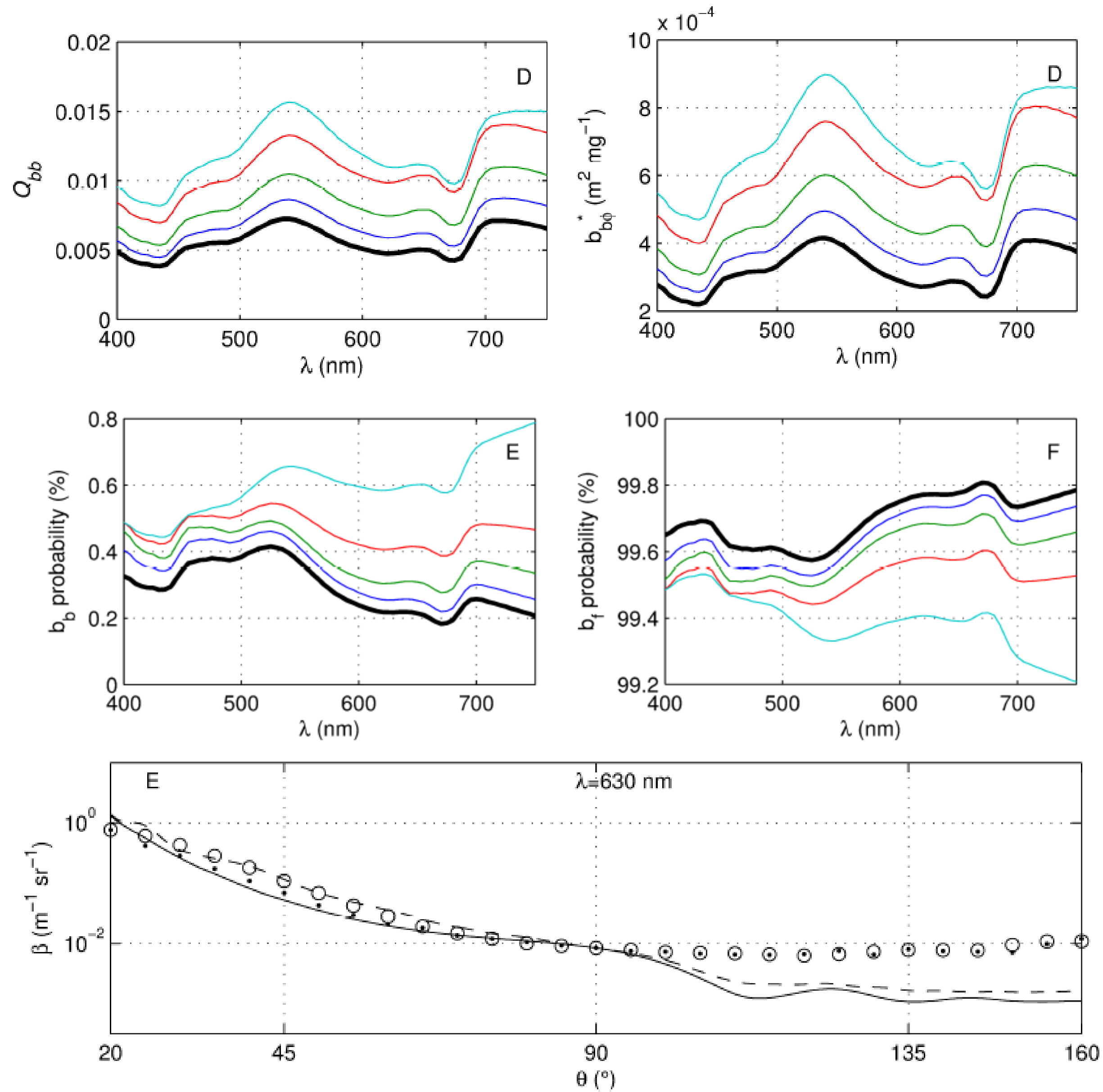

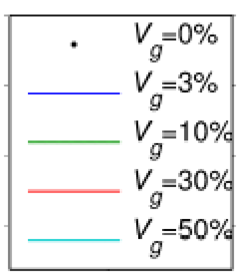

Coupled radiative transfer models: effects of gas vacuoles on reflectance

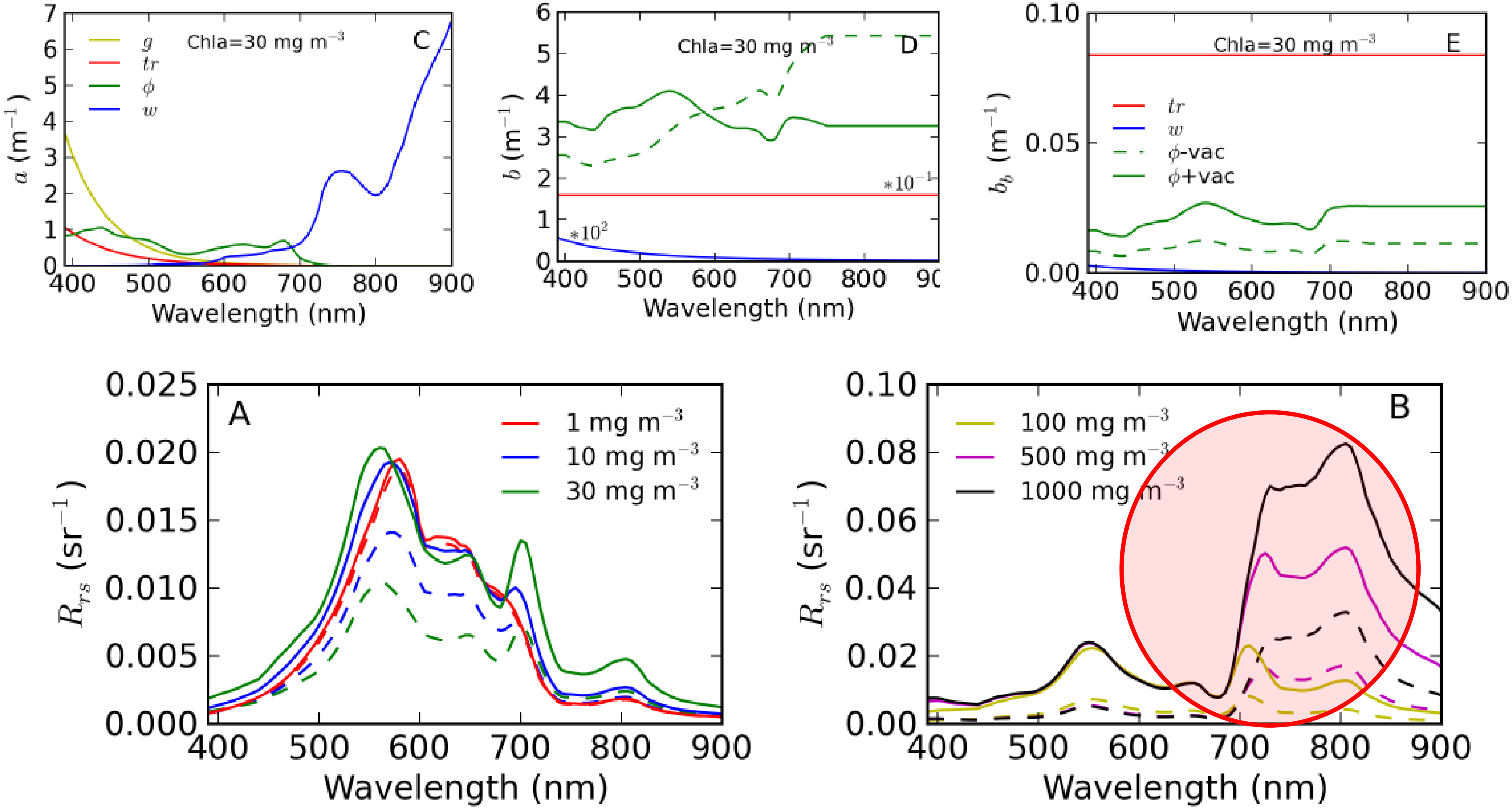

Magnitude of Rrs increased greatly (especially in red/NIR) by gas vacuolate cells. Matthews et al in prep

HAB/Phytoplankton Functional Type Applications: need for better characterisation of diversity and abundance at the appropriate scales

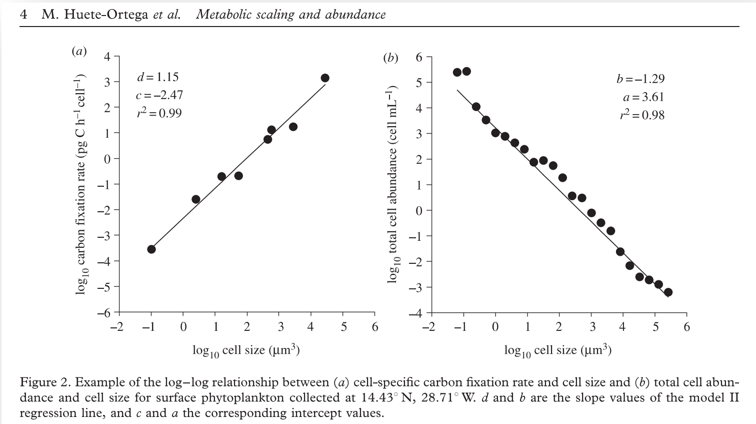

Huete-Ortega et al., 2011

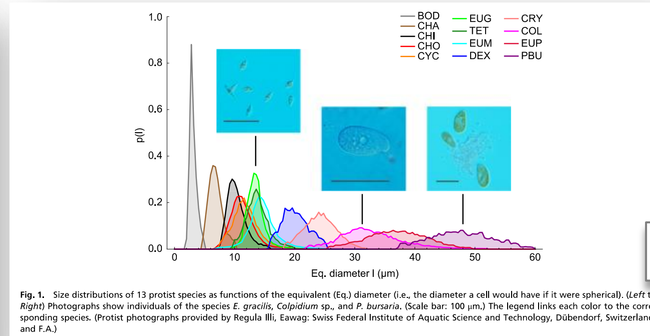

Giametto et al., 2013

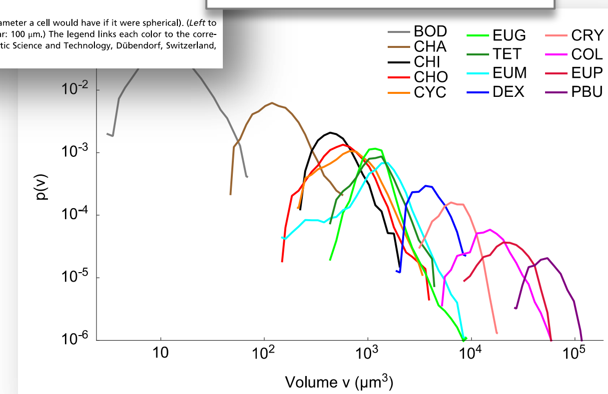

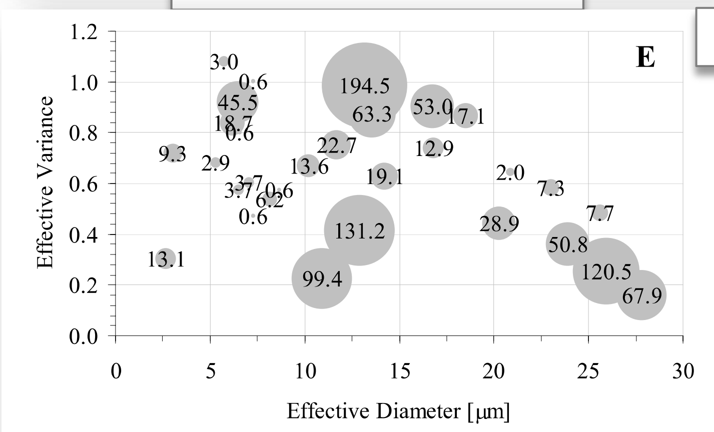

Bernard et al., 2006

Current sensitivity studies for PFT applications are limited by a lack of systematic knowledge of phytoplankton community structure across ecosystems. Our ability to model is constrained by lack of biophysical knowledge e.g. size distributions, phytoplankton counts, and resulting diversity analyses.

In the coastal & inland environment, PFT approaches based on global trophic structures are unlikely to function optimally. Abundance based empirical approaches must be regionally derived. Bio-physical approaches offer much better potential scaleability across ecosystems but systematic gathering of community structure data at the event scale are needed e.g. imaging flow cytometers, genetic probes etc….

Need for better characterisation of diversity and abundance at the appropriate scales: an example of the type of data we aspire to…..

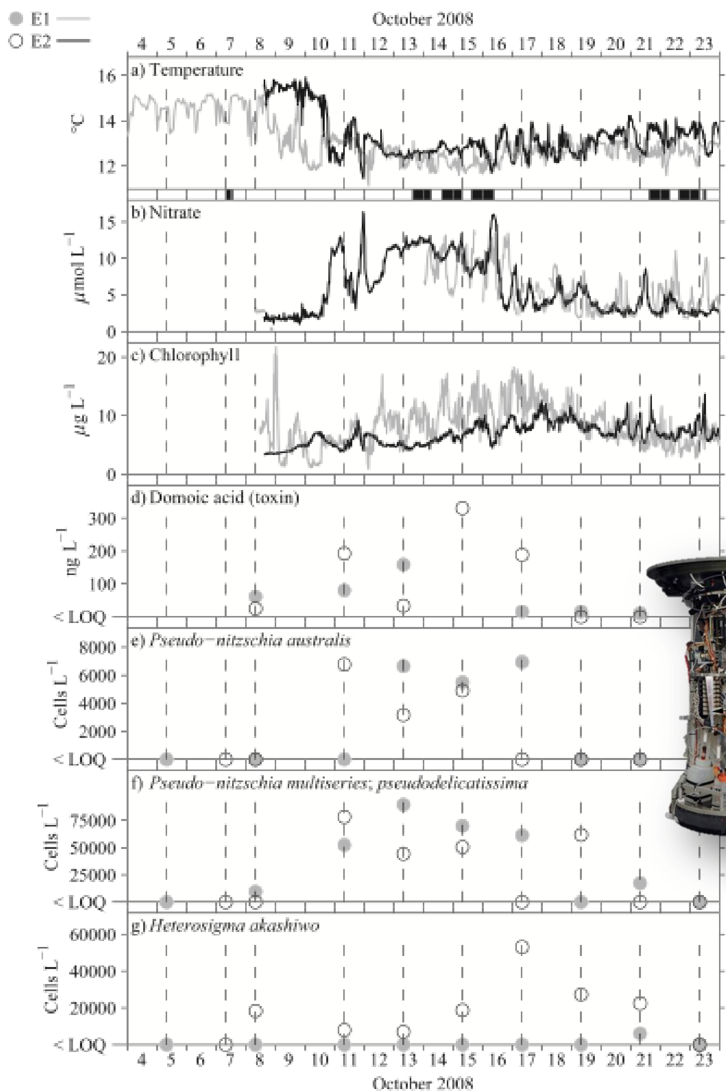

Fig. 5. (a–c) ESP environmental data (20-min resolution) and (d–g) HAB detection results at both ESP network nodes during the 2008 experiment. All environmental data are from sensors co-located with ESP, except E1 temperature during 04–07 October, which is from mooring M0 at 10-m depth (500 m west of E1). The label <LOQ indicates below the level of quantification for the ESP molecular probes. The filled periods (horizontal bars) between the temperature and nitrate plots indicate the times of AUV surveys (Fig. 15).

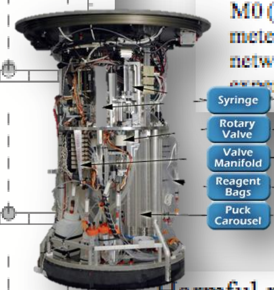

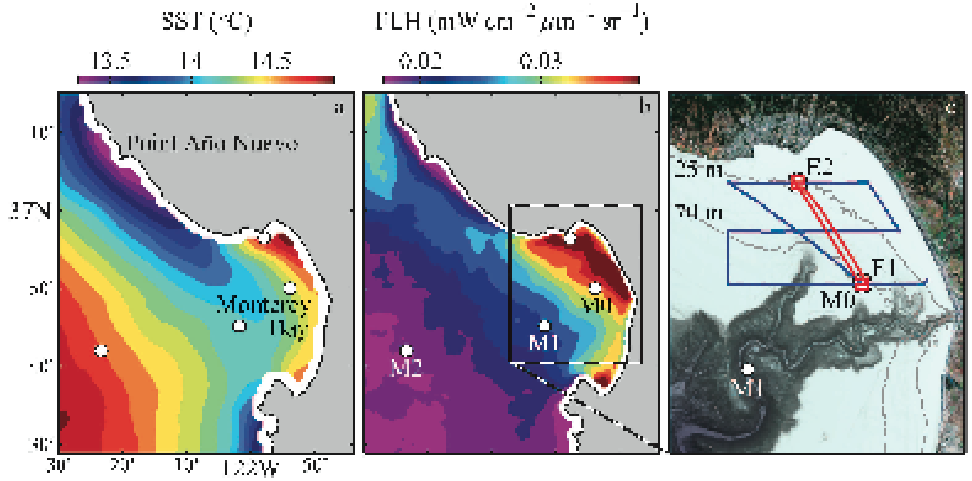

Fig. 1. Environmental setting and ESP network experiment design. Satellite-observed (a) SST and (b) chlorophyll FLH are climatologies of August–November data from 2003–2008. Moorings M0 (70-m water depth), M1 (1200-m water depth), and M2 (1800-m water depth) provided regional meteorological and oceanographic data. (c) Bathymetry in the bay is shown relative to the ESP network node locations E1 and E2 and the AUV survey tracks during the 2007 (blue) and 2008 (red) experiments. The isobaths on which E1 and E2 were placed are contoured and labeled.

Harmful phytoplankton ecology studies using an autonomous molecular analytical and ocean observing network

J. Ryan,[a,*] D. Greenfield,[b] R. Marin, III,[a] C. Preston,[a] B. Roman,[a] S. Jensen,[a] D. Pargett,[a] J. Birch,[a] C. Mikulski,[c] G. Doucette,[c] and C. Scholin[a]

[a] Monterey Bay Aquarium Research Institute, Moss Landing, California
[b] University of South Carolina, Charleston, South Carolina
[c] National Oceanic and Atmospheric Administration, National Ocean Service, Charleston, South Carolina

Abstract

Using autonomous molecular analytical devices embedded within an ocean observatory, we studied harmful algal bloom (HAB) ecology in the dynamic coastal waters of Monterey Bay, California. During studies in 2007 and 2008, HAB species abundance and toxin concentrations were quantified periodically at two locations by Environmental Sample Processor (ESP) robotic biochemistry systems. Concurrently, environmental variability and processes were characterized by sensors co-located with ESP network nodes, regional ocean moorings, autonomous underwater vehicle surveys, and satellite remote sensing. The two locations differed in their long-

Ocean colour applications in coastal and inland waters: Need for optimised in-situ measurements & protocols

Algorithm development and testing is dependent upon the availability of high quality *in situ* data, as is radiometric and further geophysical validation.

Standardisation of protocols necessary for the development of globally-representative data sets, with (ideally) known error products for the geophysical, inherent optical properties, apparent optical properties, and atmospheric properties required.

While coastal seas are well represented in current data sets e.g. NOMAD, cohesive data from more bio-optically challenging coastal and (particularly) inland waters are scarce.

With increasing interest in coastal and inland applications, there is a need to establish protocols that enable standardised development of the necessary algorithm parameterisation and validation data sets....

Building on available protocols – what spatial differences must we account for?

Fig. 4. A part (37.6 × 57.2 km) of a true color image
vanced Land Imager (ALI) acquired on 14 July 2002 in th
western part of the Gulf of Finland. Areas in which pres
surface scums was estimated using band 4 (775–805 nm) refl
values are shown in red. The Hyperion footprint seen in F
indicated with the frame.

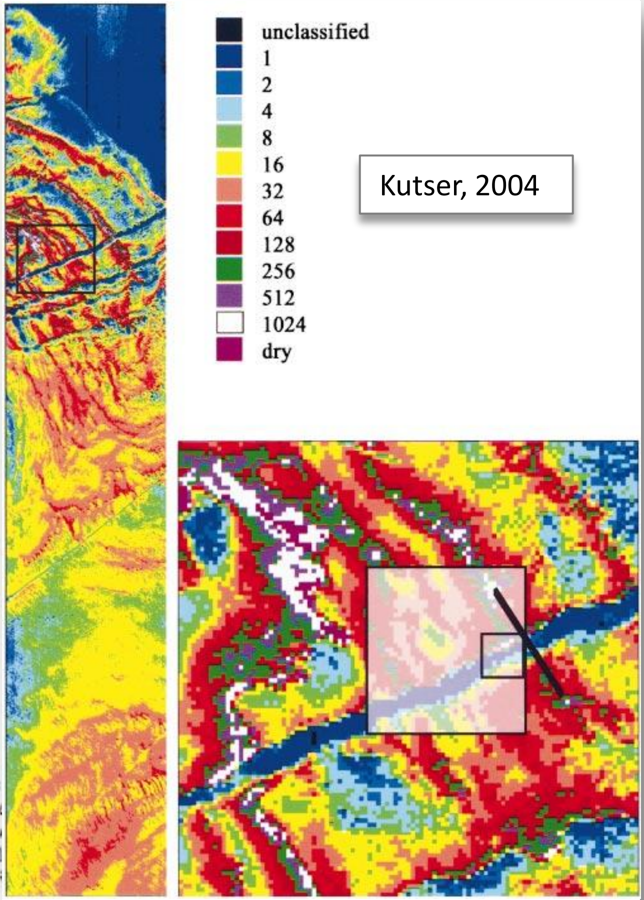

Kutser, 2004

Fig. 5. Chlorophyll map of the northwestern part of the Gulf of Finland and the zoom-in area with the ship track under investigation. Modeled spectral library and Spectral Angle Mapper with a maximum angle of 0.5 rad were used to classify the image. Numbers in the legend indicate chlorophyll *a* concentrations in mg m^{-3} corresponding to each class. The transect across a ship track (thick black line) and areas equal to 1 × 1 km and 240 × 270 m hypothetical satellite pixels, used in the analysis, are indicated in the zoom image. Size of the area shown in the Hyperion image is 7 × 42.3 km.

High spatial variability at high biomass affect stability to concurrently make multi-parameter in situ measurements consistently, and results in sub-pixel variability for satellite match-ups....

Building on available protocols – new methods needed for high biomass spatial variability?

Impact of sub-pixel variations on ocean color remote sensing products

Zhongping Lee,[1,*] Chuanmin Hu,[2] Robert Arnone,[3] and Zhen Liu[1]

[1] *Department of Environmental, Earth and Ocean Sciences, University of Massachusetts, Boston, Massachusetts 02125, USA*

[2] *College of Marine Science, University of South Florida, St. Petersburg, Florida 33701, USA*

[3] *Naval Research Laboratory, Stennis Space Center, Mississippi 39529, USA*

**Zhongping.lee@umb.edu*

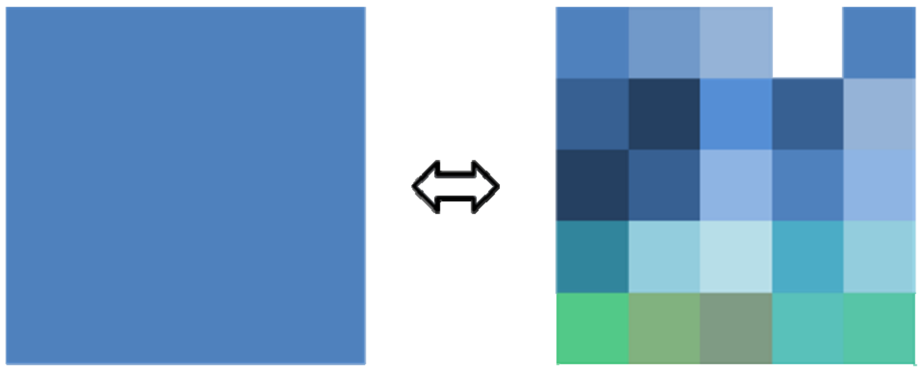

Fig. 1. (left) A pixel observed by a low-resolution sensor; (right) Pixels observed by a high-resolution sensor, corresponding to the low-resolution pixel.

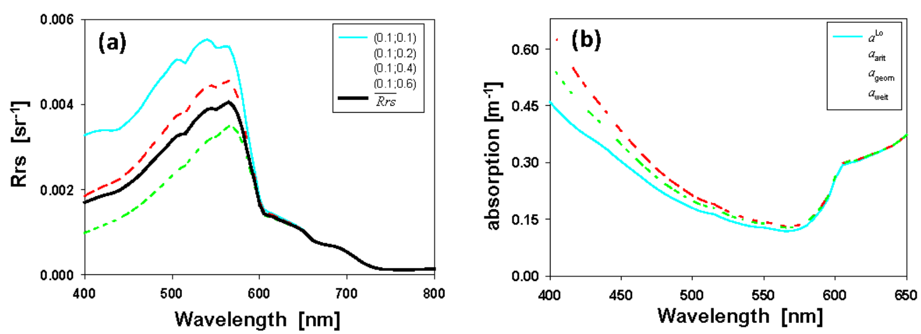

Fig. 2. (a) *Rrs* of 4 high-resolution pixels and their average. First value and second value in the parenthesis are the absorption coefficient of phytoplankton and CDOM at 440 nm, respectively. (b) Absorption spectrum derived from the average *Rrs* (blue line), as compared with the average absorption spectra using various schemes, including arithmetic mean, geometric mean, and backscattering-weighted mean (Eq. (8)).

Building on available protocols – what depth differences must we account for?

...stratification, thin layers and motility, challenging to resolve both from a sampling perspective and with regard to their effects on the water leaving radiance....

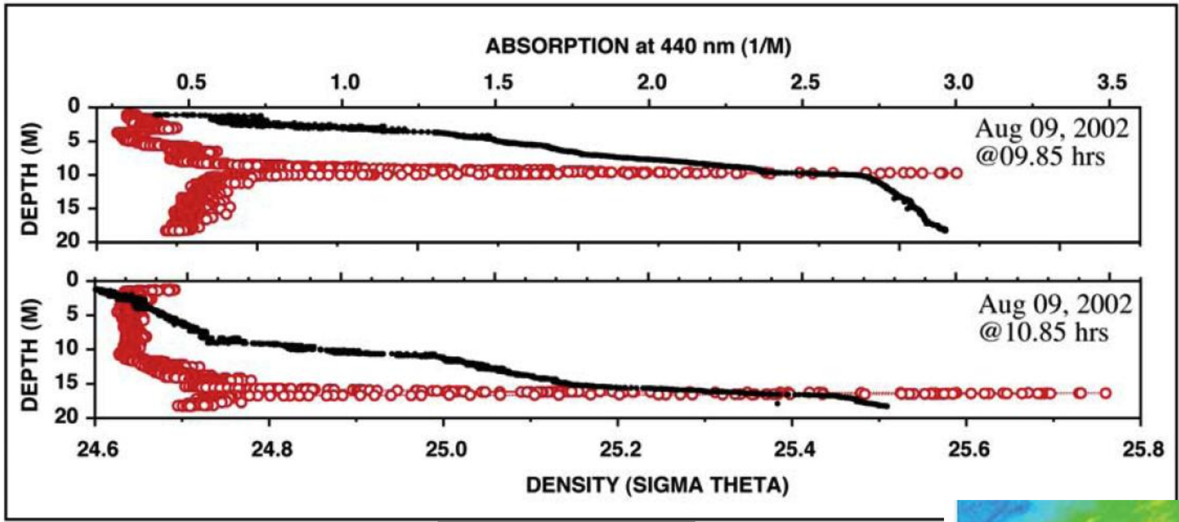

Babin et al, 2005

Courtesy Raphe Kudela

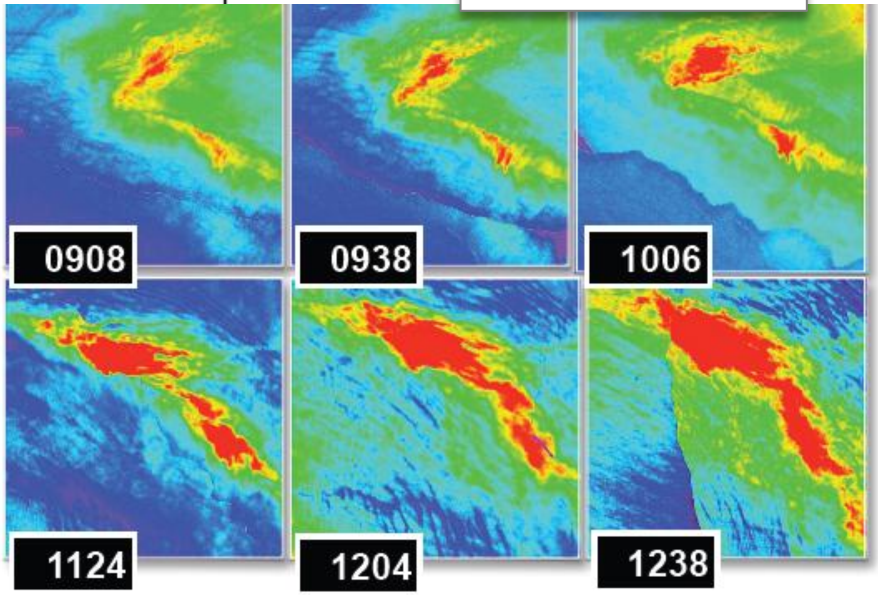

Building on available protocols – what depth differences must we account for?

Baltic sea optical depth (extremely shallow in blue) poses challenges for coupling remote and in situ observation networks….

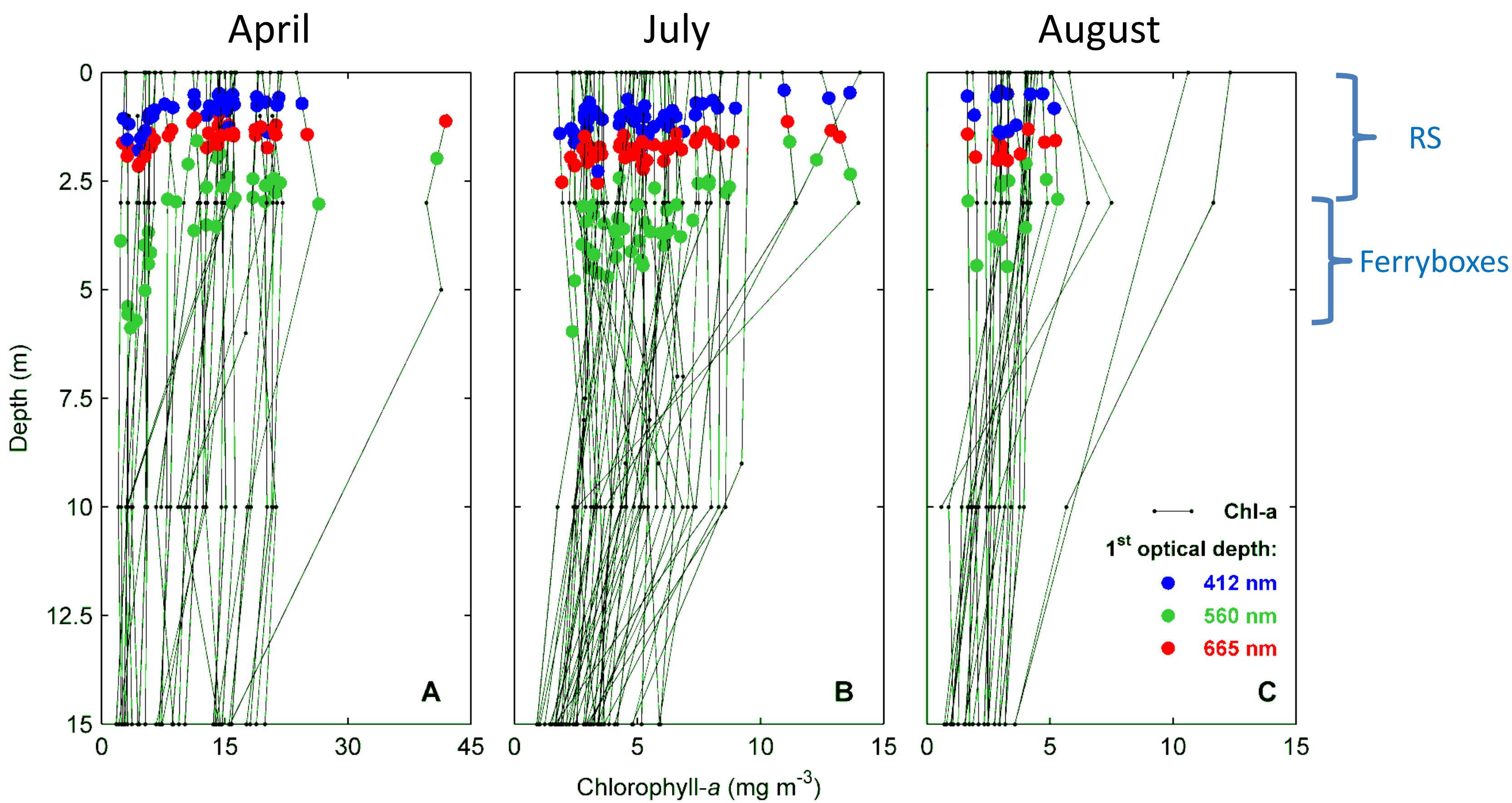

Simis et al. *in prep*

Coupled radiative transfer models: improving understanding of measurement constraints for highly turbid waters

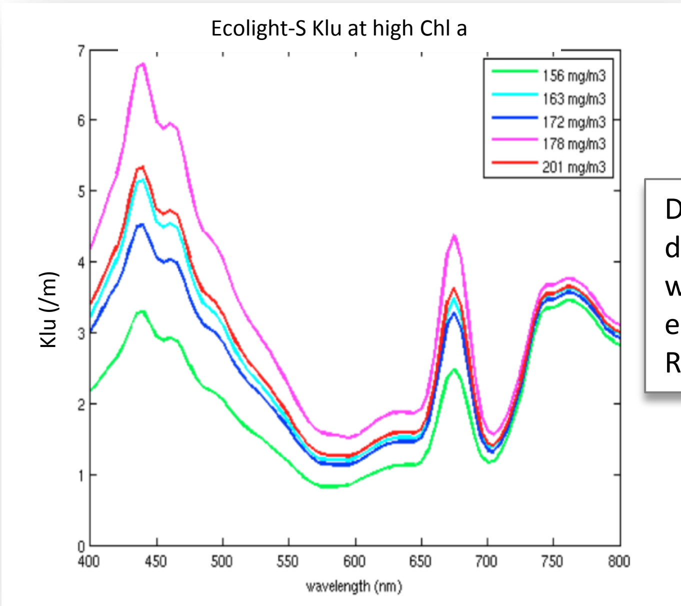

Demonstrating the demands upon in-water radiometry in eutrophic waters. Robertson et al in prep

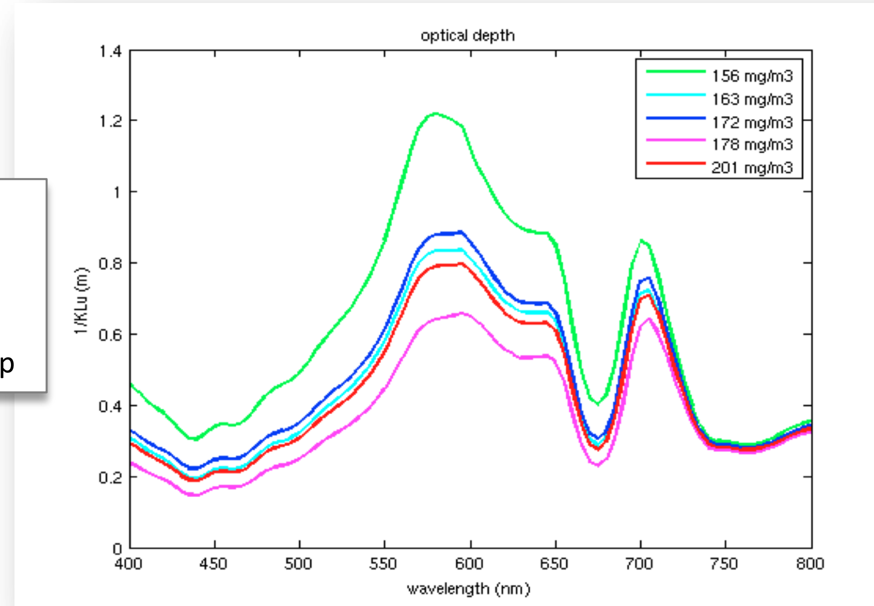

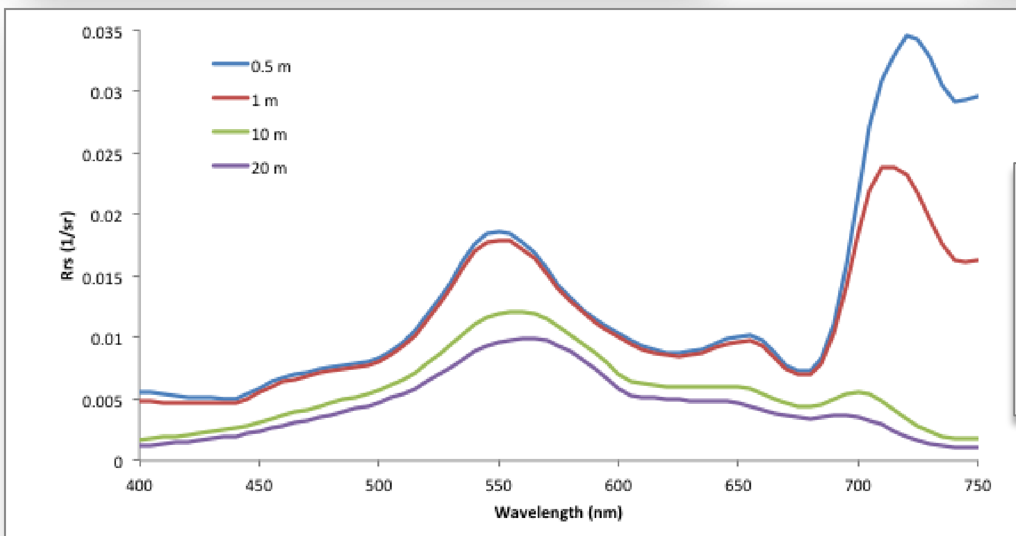

Phytoplankton constant areal biomass = 200 mg m^-2 with variable depth layer from surface
Phytoplankton contained in surface layer only, and excluded from layer below
Depth of surface layer is 0.5 m, 1 m, 10 m, 20 m.
Matthews et al IOCCG/GEHAB in prep

Building on available protocols – what IOP differences must we account for?...or trying to force green slime through optical flow tubes at the wrong depth scales

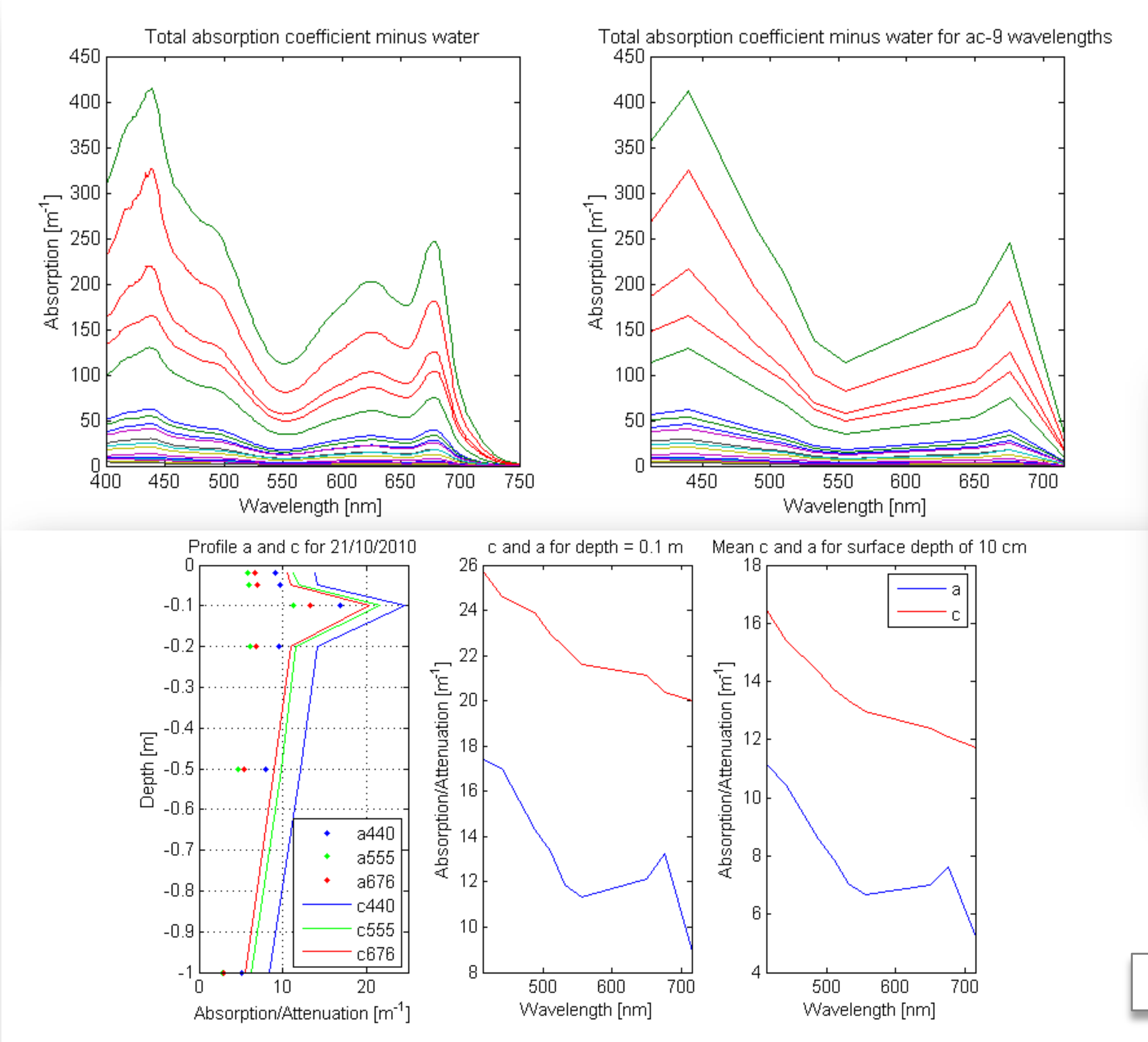

Figure 12: Selected depth profiles and depth-specific wavelength plots of a and c from an ac-9 meter

Matthews, unpublished

The elephant in the room? Atmospheric correction and adjacency effects for turbid waters inconveniently close to land….

- The atmospheric correction issues facing ocean colour use in coastal and inland waters are considerable: highly turbid waters, the problems of adjacency, complex aerosol contributions, etc.
- See splinter session summary on advances in atmospheric correction (including turbid waters) for the well-informed consensus…..
- Consideration of alternative atmospheric corrections algorithms necessary, particularly for small water bodies.

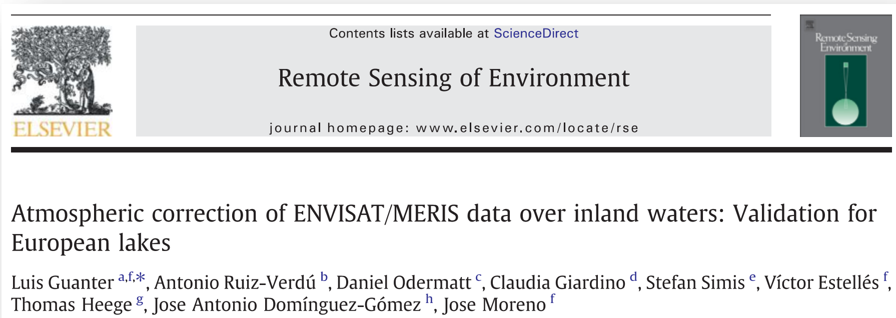
Contents lists available at ScienceDirect

Remote Sensing of Environment

journal homepage: www.elsevier.com/locate/rse

Atmospheric correction of ENVISAT/MERIS data over inland waters: Validation for European lakes

Luis Guanter [a,f,*], Antonio Ruiz-Verdú [b], Daniel Odermatt [c], Claudia Giardino [d], Stefan Simis [e], Víctor Estellés [f], Thomas Heege [g], Jose Antonio Domínguez-Gómez [h], Jose Moreno [f]

"…As an alternative to these methods, the SCAPE-M atmospheric processor is proposed in this paper for the automatic atmospheric correction of ENVISAT/MERIS data over inland waters. A-priori assumptions on the water composition and its spectral response are avoided by SCAPE-M by calculating reflectance of close-to-land water pixels through spatial extension of atmospheric parameters derived over neighboring land pixels…"

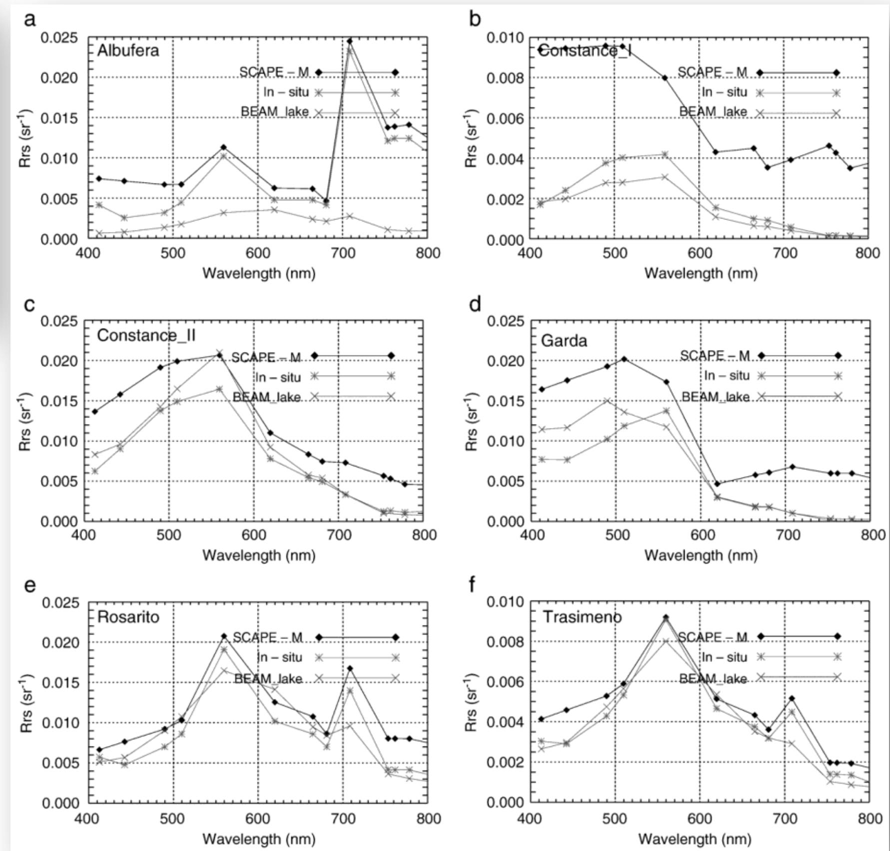

Fig. 5. Comparison between reflectance spectra calculated by SCAPE-M and the BEAM lake processors. All the data were processed by ICOL and C2R processors in BEAM, except for Lake Albufera and Lake Rosarito, to which the *eutrophic lakes* processor was applied.

Algorithm examples: top-of-atmosphere eutrophication/cyanobacterial algorithms

Contents lists available at ScienceDirect

Remote Sensing of Environment

journal homepage: www.elsevier.com/locate/rse

ELSEVIER

A novel ocean color index to detect floating algae in the global oceans

Chuanmin Hu *

College of Marine Science, University of South Florida, 140 Seventh Avenue, South, St. Petersburg, FL 33701, United States

floating algae. Therefore, the Floating Algae Index is defined as:

$$\mathrm{FAI} = R_{\mathrm{rc,NIR}} - R'_{\mathrm{rc,NIR}},$$
$$R'_{\mathrm{rc,NIR}} = R_{\mathrm{rc,RED}} + \left(R_{\mathrm{rc,SWIR}} - R_{\mathrm{rc,RED}}\right) \times (\lambda_{\mathrm{NIR}} - \lambda_{\mathrm{RED}}) / (\lambda_{\mathrm{SWIR}} - \lambda_{\mathrm{RED}}), \quad (4)$$

where $R'_{\mathrm{rc,NIR}}$ is the baseline reflectance in the NIR band derived from a linear interpolation between the red and SWIR bands. Note that the definition of FAI is similar to that for MODIS FLH (Fluorescence Line Height, Letelier & Abott, 1996) and MERIS MCI (Gower et al., 2005), but uses different band combination. In the above equations for

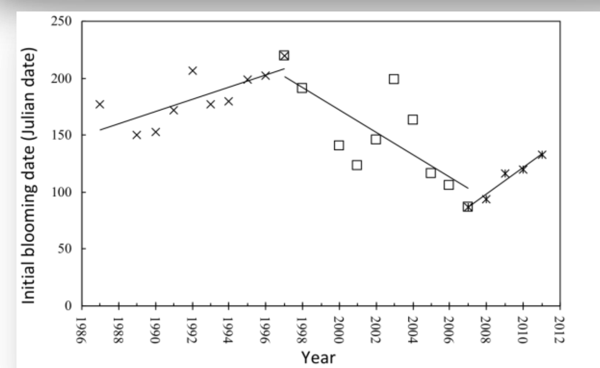

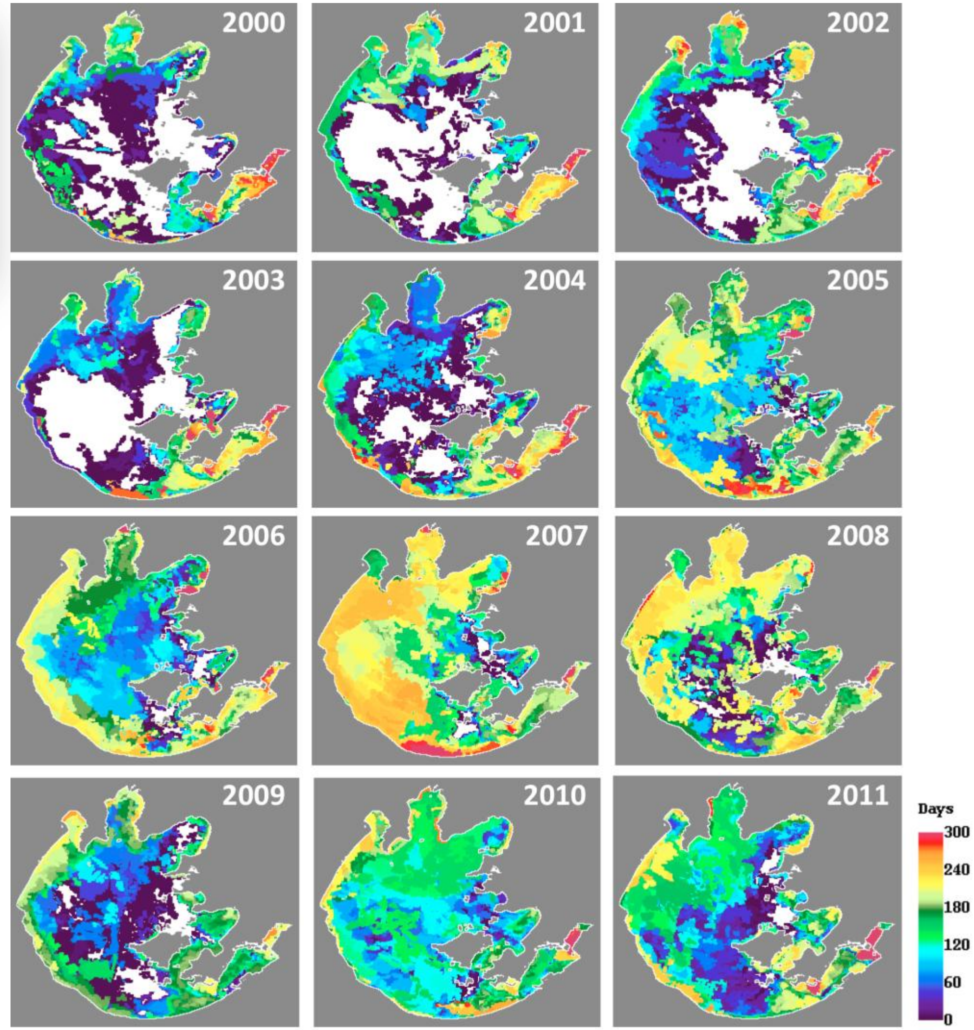

Figure 1 Duration of cyanobacteria blooms, defined as the period between the first and last day with FAI > -0.004 in the MODIS imagery. White areas showed no bloom during the entire year.

Hu et al 2012, IOCCG/GEOHAB in prep

Algorithm examples: top-of-atmosphere eutrophication/cyanobacterial algorithms

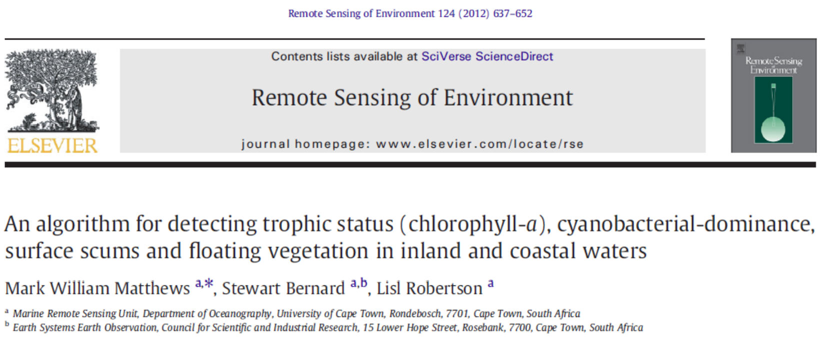

Remote Sensing of Environment 124 (2012) 637–652

Contents lists available at SciVerse ScienceDirect

Remote Sensing of Environment

journal homepage: www.elsevier.com/locate/rse

An algorithm for detecting trophic status (chlorophyll-*a*), cyanobacterial-dominance, surface scums and floating vegetation in inland and coastal waters

Mark William Matthews [a,*], Stewart Bernard [a,b], Lisl Robertson [a]

[a] Marine Remote Sensing Unit, Department of Oceanography, University of Cape Town, Rondebosch, 7701, Cape Town, South Africa
[b] Earth Systems Earth Observation, Council for Scientific and Industrial Research, 15 Lower Hope Street, Rosebank, 7700, Cape Town, South Africa

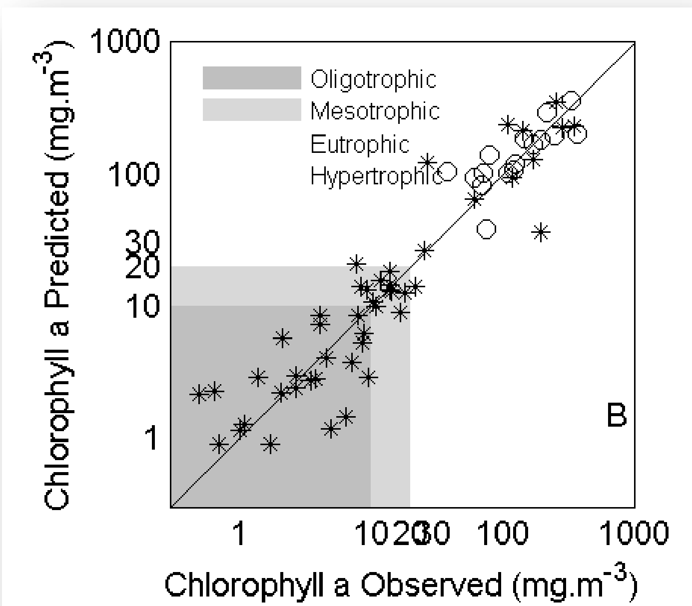

Maximum Peak Height Algorithm

Chlorophyll-a empirically based algorithm designed for trophic state / cyanobacteria detection in inland and near-coastal phytoplankton-dominant waters

Based on the Maximum Peak Height (MPH) in the MERIS red bands at 681, 709 and 753 nm

Utilizes MERIS BRR (not Rrs) to normalize for atmospheric Rayleigh effects because of problems with atmospheric corrections

Simultaneously handles 3 primary cases:

Mixed oligotrophic/mesotrophic low to medium biomass conditions with Chl-a less than 30 mg.m-3 ⍰ 681 fluorescence

- 1.a eukaryote species SICF signal
- 1.b special case: low biomass cyanobacterial blooms (no SICF)

High biomass or eutrophic/hypertrophic water with Chl-a concentrations greater than 30 mg.m-3 ⍰ 709 backscatter

- 2.a eukaryote species (Diatoms/Dinoflagellates)
- 2.b vacuolate cyanobacterial species

Extremely high biomass conditions associated with surface scums, or hyperscums, and ‘dry’ floating algae or vegetation (Chl-a > 500 mg.m-3)

- Cyanobacterial scums (chl-a > 500 mg.m^(-3))

Algorithm options: top-of-atmosphere eutrophication/cyanobacterial algorithm

Global examples | South African examples

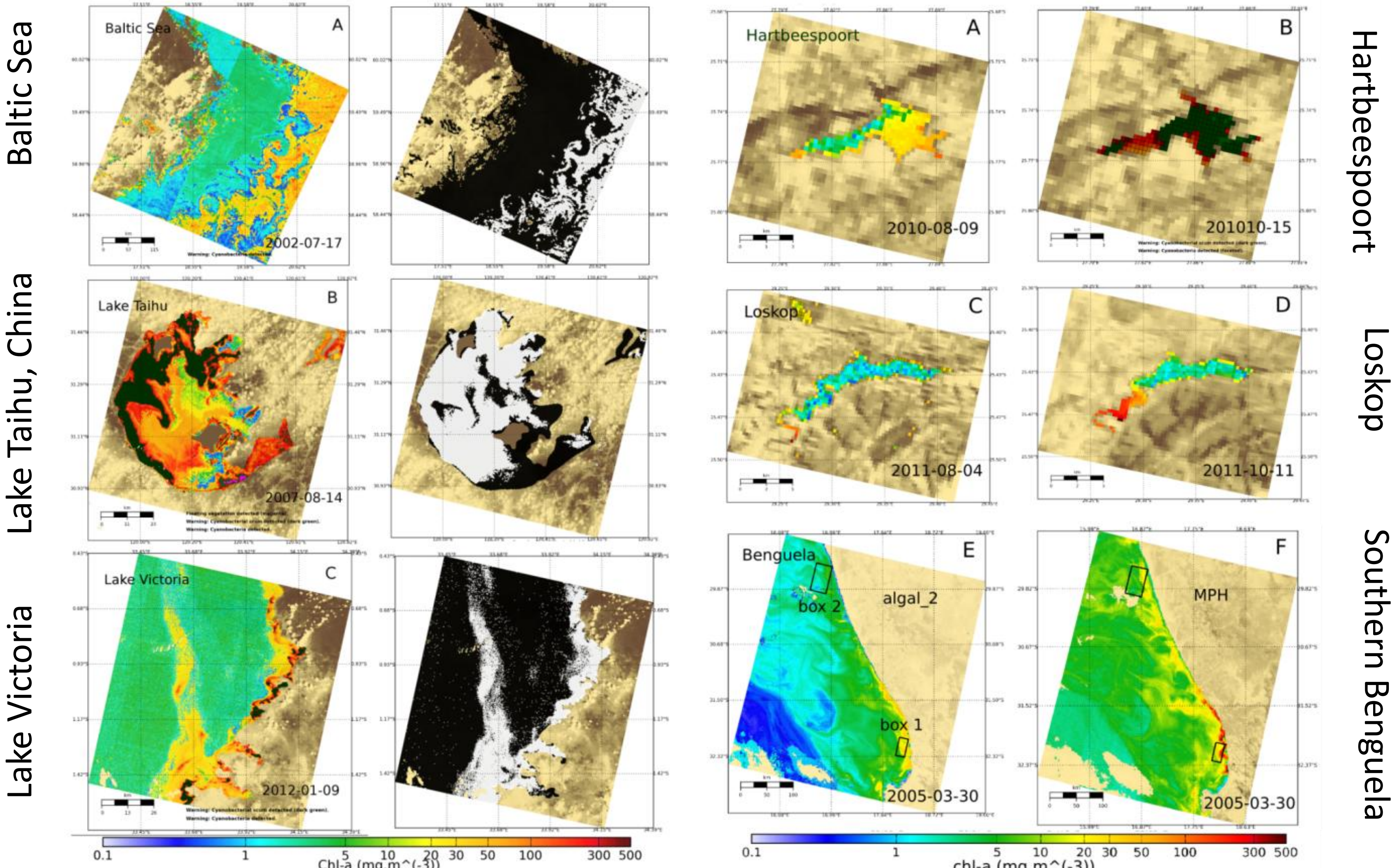

Matthews IOCCG/GEOHAB in prep

Phenological applications of the MPH algorithm: ten years of cyanobacteria

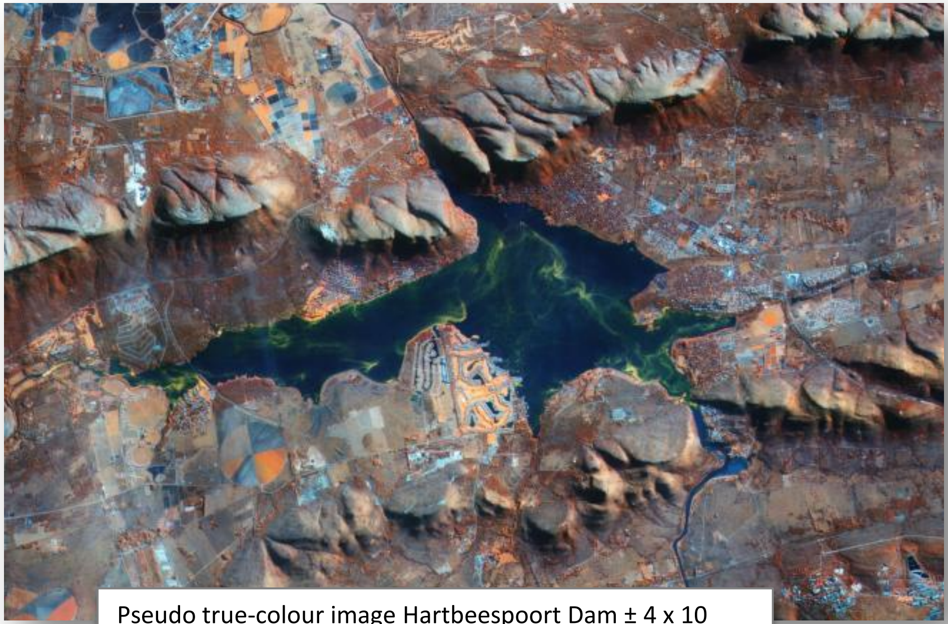

Pseudo true-colour image Hartbeespoort Dam ± 4 x 10 km, SumbandilaSat, May 2010. Meyer, unpublished

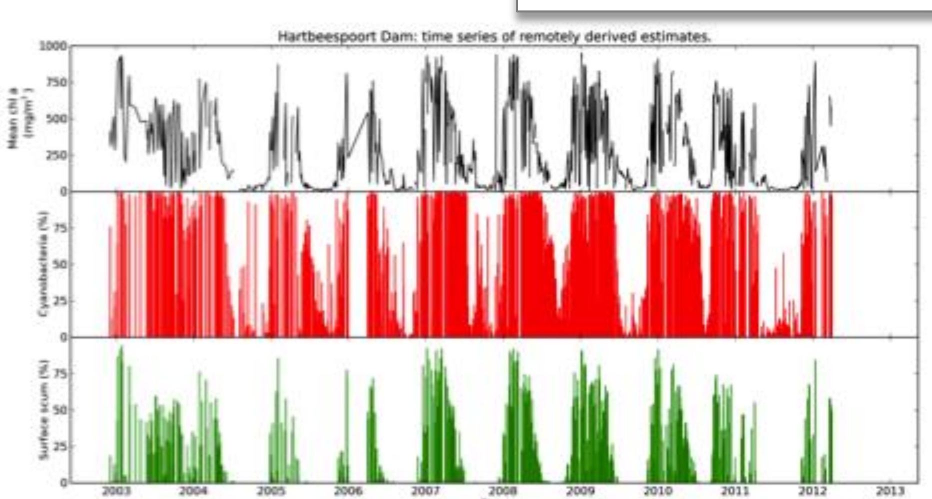

10 year time series of phytoplankton biomass (top), percentage cyanobacteria (middle), and percentage surface scums (bottom) for Hartbeespoort Dam, using the MPH algorithm applied to MERIS FR data. Matthews IOCCG/GEOHAB in prep

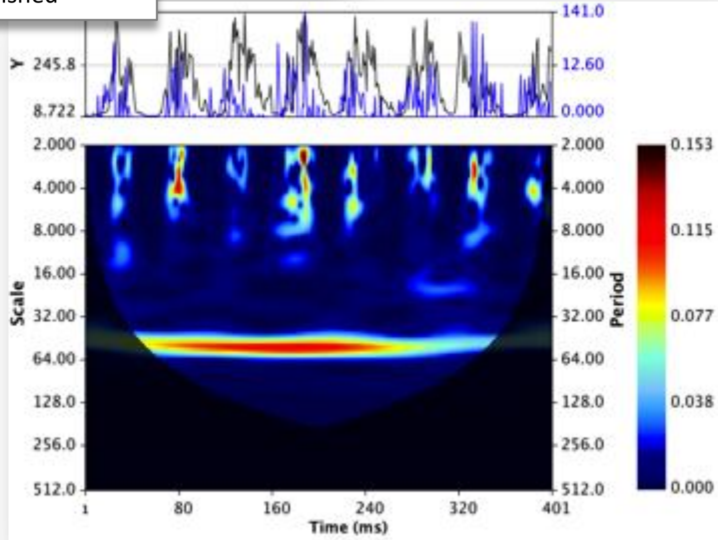

X-wavelet analysis of phytoplankton biomass vs precipitation for the same Hartbeespoort time. Pienaar et al in prep

Algorithm examples: simple empirical algorithms for biomass estimates in eutrophic waters

IOP Publishing — Environmental Research Letters
Environ. Res. Lett. 4 (2009) 045003 (5pp) — doi:10.1088/1748-9326/4/4/045003

A bio-optical algorithm for the remote estimation of the chlorophyll-*a* concentration in case 2 waters

Anatoly A Gitelson, Daniela Gurlin, Wesley J Moses and Tadd Barrow

The same model (equation (2)) was used to assess the potential of MODIS and MERIS to retrieve the chl-*a* concentration in turbid productive waters.

We tested the model in the form

$$\mathrm{MODIS}_{2\mathrm{band}} = R_{15}/R_{13} \quad (4)$$

$$\mathrm{MERIS}_{3\mathrm{band}} = (R_7^{-1} - R_9^{-1}) \times R_{10} \quad (5)$$

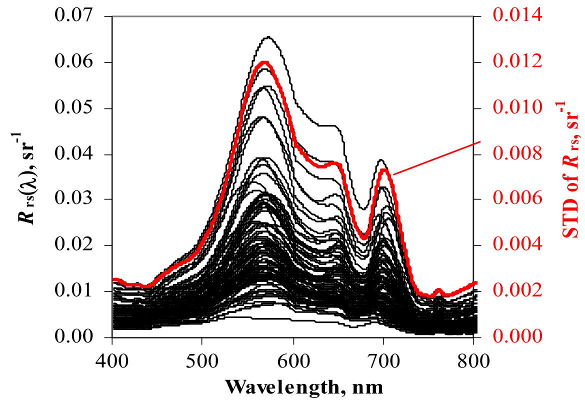

Figure 2. Remote-sensing reflectance, R_{rs}, spectra and spectrum of their standard deviation, STD (in red, right axis).

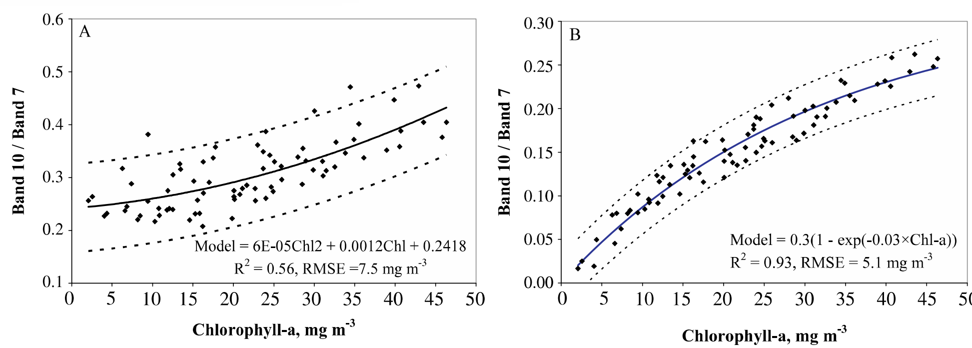

Figure 5. Two-band model values with simulated MODIS bands (A), and three-band model values with simulated MERIS bands (B), versus chl-*a* concentrations.

Algorithm examples: IOP range based detection of *Karenia brevis*

A novel technique for detection of the toxic dinoflagellate, Karenia brevis, in the Gulf of Mexico from remotely sensed ocean color data

Jennifer P. Cannizzaro[a,*], Kendall L. Carder[a], F. Robert Chen[a], Cynthia A. Heil[b], Gabriel A. Vargo[a]

[a]College of Marine Science, University of South Florida, St. Petersburg, FL 33701, USA
[b]Florida Fish and Wildlife Conservation Commission, Fish and Wildlife Research Institute, St. Petersburg, FL 33701, USA

Received 22 May 2003; received in revised form 7 January 2004; accepted 15 April 2004
Available online 25 September 2007

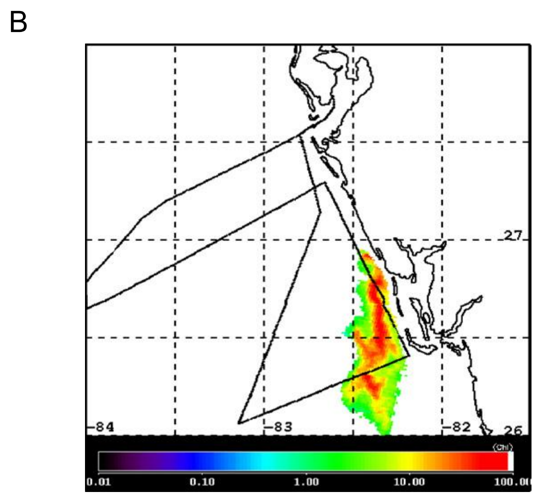

Fig. 11. (A) Surface in situ chlorophyll concentrations versus FLH data derived from shipboard $R_{rs}(\lambda)$ data. Symbol size increases with increasing *K. brevis* cell concentrations (cells l^{-1}). Regression lines for cell concentrations less than 10^4 cells l^{-1} (solid) and greater than 10^4 cells l^{-1} (dashed) were obtained by least-squares linear regression on log-transformed data. Only data with FLH's greater than 0.1 W m^{-2} μm^{-1} sr^{-1}, equivalent to Chl ~1 mg m^{-3}, were regressed. (B) MODIS FLH data of the WFS acquired on 30 August 2001 converted to Chl (mg m^{-3}) using the relationship derived for cell concentrations greater than 10^4 cells l^{-1}. Only the region positively flagged for *K. brevis* is quantified.

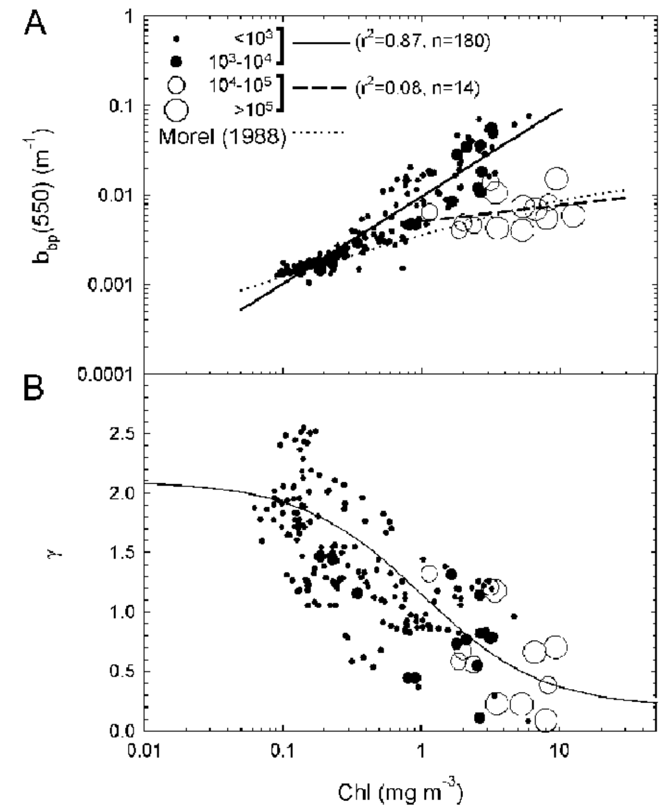

Fig. 6. (A) Relationship between Chl and particulate backscattering at 550 nm for surface data collected on the WFS in 2000 and 2001. Symbol size increases with increasing K. brevis cell concentrations (cells l^{-1}). Regression lines for cell concentrations less than 10^4 cells l^{-1} (solid) and greater than 10^4 cells l^{-1} (dashed) were obtained by least-squares linear regression on log-transformed data. An empirical relationship determined by Morel (1988) for modeled Case 1 data (dotted) is shown for comparison. (B) Relationship between Chl and the b_{bp}(l) spectral shape parameter, g. An empirical function (solid) developed for all K. brevis cell concentrations is shown.

Algorithm examples: semi-analytical phytoplankton functional type for effective diameter

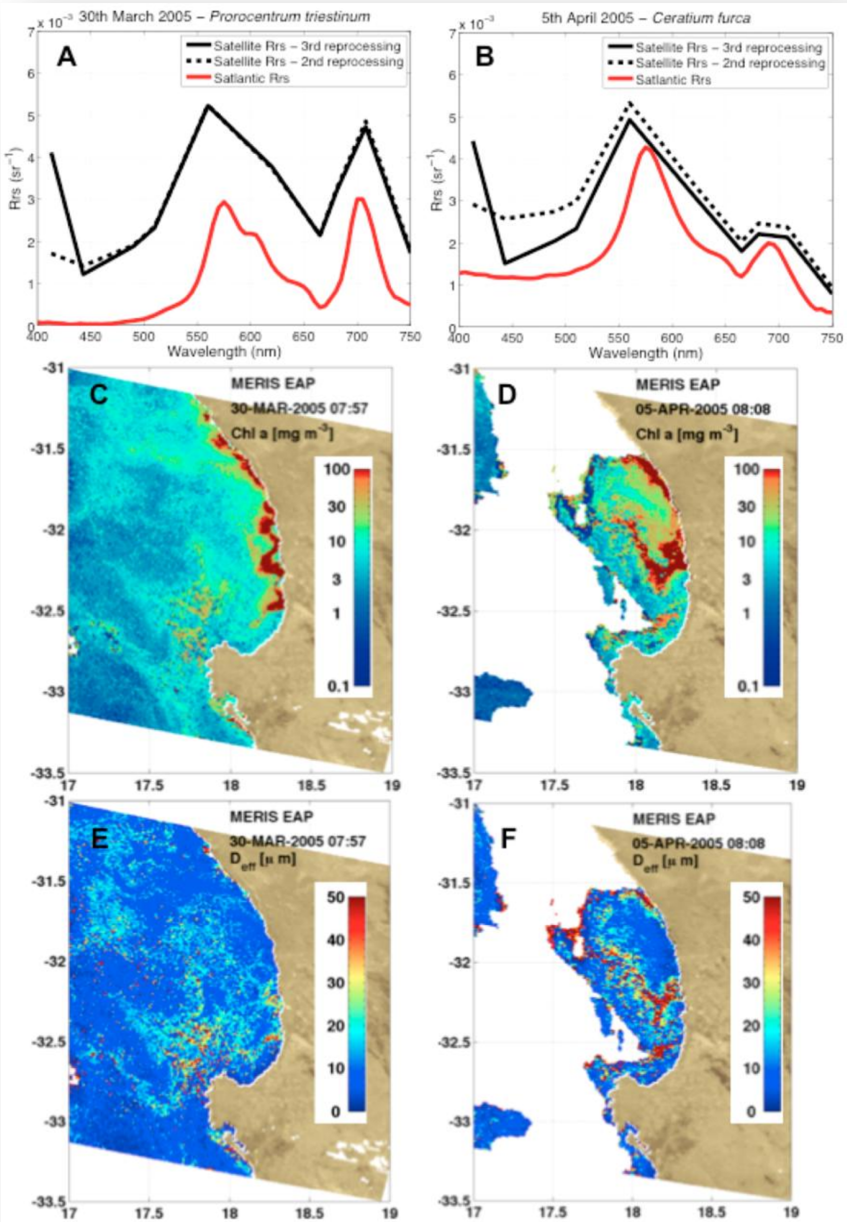

MERIS Reduced Resolution radiometric match-ups (A and B); and algorithm outputs from the Equivalent Algal Population semi-analytical algorithm, demonstrating the effectiveness of this approach for detecting high biomass (C and D) and distinguishing dominance by small (Prorocentrum triestinum) and large (Ceratium furca) dinoflagellates (E and F respectively) using the effective diameter product. Bernard et al in press, IOCCG/GEOHAB

Algorithm inter-comparisons for a wide variety of coastal waters

coastcolour	Doc:	CCRRreport.doc		
	Date:	21.12.2012		
	Issue:	2	Revision: 2	Page 55

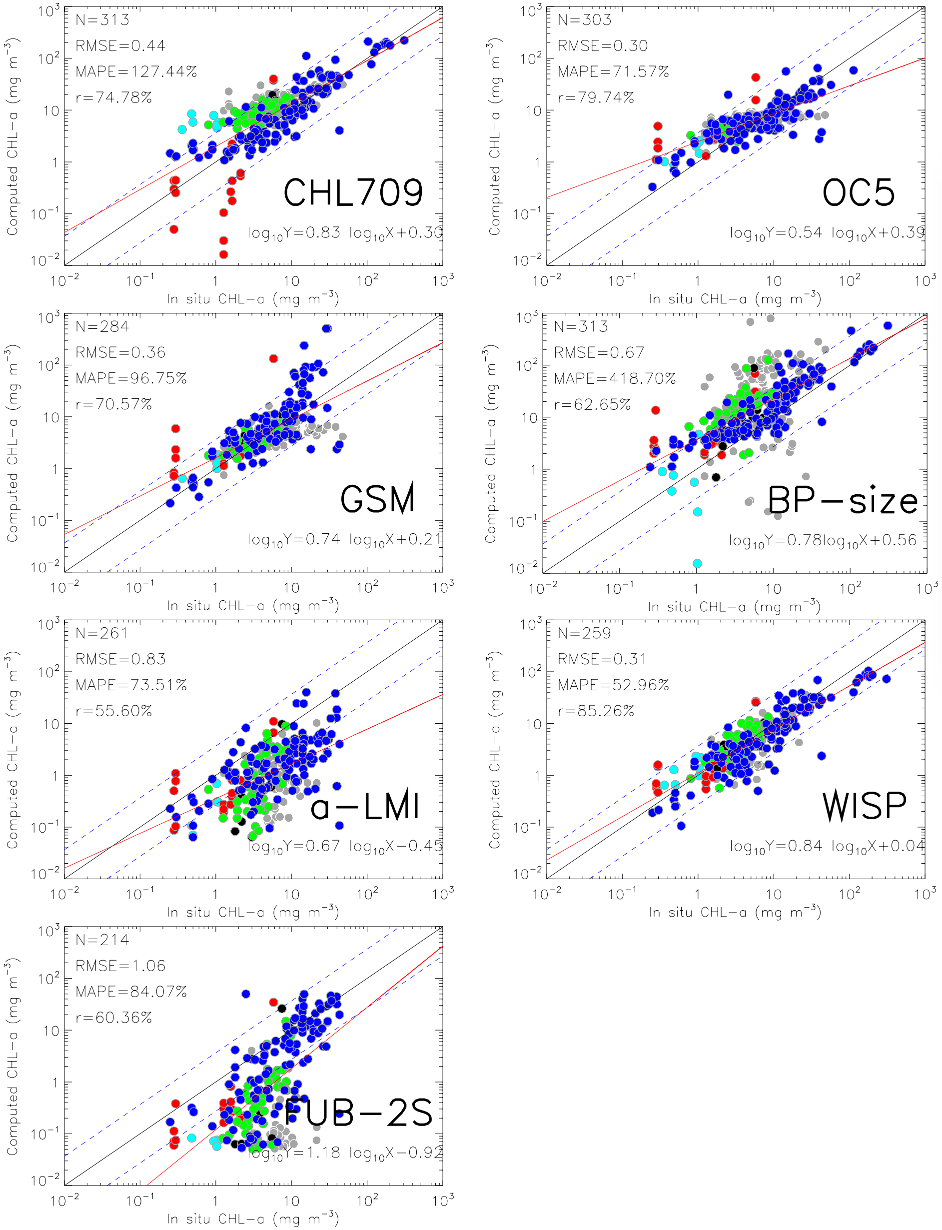

Figure 26: CHL concentrations (mg m^{-3}) estimated by the algorithms indicated in the figures, versus in situ CHL from Dataset 2.

coastcolour

DUE CoastColour

Round Robin ▫ Harmonised comparison of algorithms

Further developments through the IOCCG-CWAC (Coastal Water Algorithm Comparison) Working Group

Spectral classification techniques: system-transferable, scaleable algorithm structures

- There is necessity to describe a considerable amount of variability in Inherent Optical Property (IOP) subcomponent models.
- This is particularly true, if inversion algorithms are to be applicable at global scale yet remain quantitatively accurate in coastal & shelf seas.
- This is unlikely to be achieved in the foreseeable future, with a single representation of IOP subcomponents.
- The proposed approach is an algorithm framework more than a specific algorithm.

Advantages of fuzzy logic defined provinces

- They allow for dynamics both seasonal and inter-annual in the optical properties of a given region.
- They address the issue of transitions at the boundaries of provinces (through the fuzzy membership function of each class) thus resulting finally in the seamless reconstruction of a single geophysical product.
- The framework structure allows for further class based selection of empirical or semi-analytical algorithms, selected bandsets, inversion type…..

Error Specification according to Optical Water Type

Spectral Radiance Values Per Pixel

Fuzzy Logic Membership in Optical Water Type

Biogeochemical and Bio-optical Products

Uncertainties, by Optical Type and by Product

Uncertainties per pixel and per product

Advantages:

- Not limited by geographic region, provided all possible optical water types are classified
- Error assignment on basis of overall optical signal, and not on a single variable, e.g. chlorophyll, and hence consistent across products
- Total number of water types is small, so number of observations per class would be greater than if we were to use a large number of class intervals
- Optical classification provides a way to distinguish case-1 and case-2 waters
- No sharp boundaries across types

Courtesy Shubha Sathyendranath, OC-CCI work, preliminary outputs

Error Specification Refinement: Fuzzy Logic

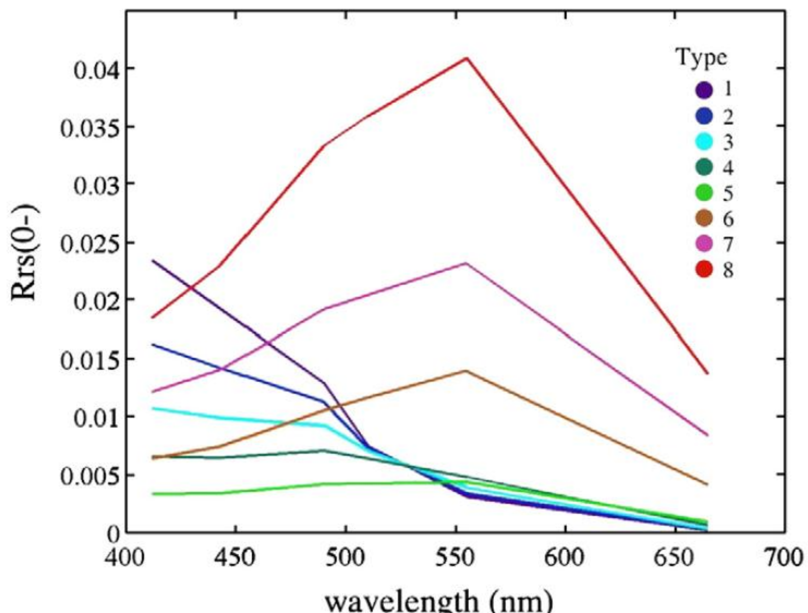

! "#$ %& ##"' %(%*+% . . / 0%1 2' ") 3' % $ #(' 45' 6576 3%
"' 8* 9() 69' % ' 9(") %4; %< ' %7 3<(%) (' "%2*) 55' 5+%

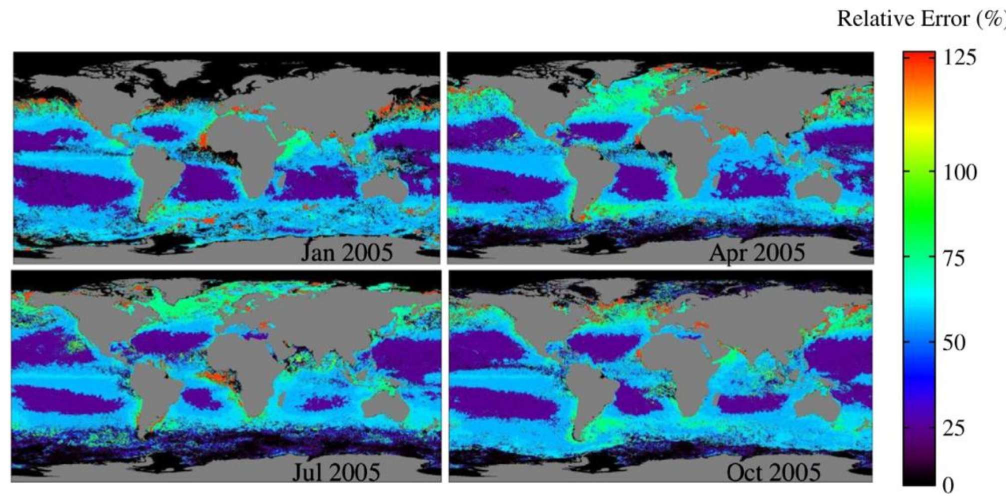

Moore et al. 2009

Courtesy Shubha Sathyendranath, OC-CCI work, preliminary outputs

Note:
Fuzzy logic also part of merging technique.
Fuzzy logic also basis of a CoastColour algorithm: Facilitate meeting of Case -1 and Case-2 algorithms in the future

Spectral classification for Case 2 waters: application at a variety of scales

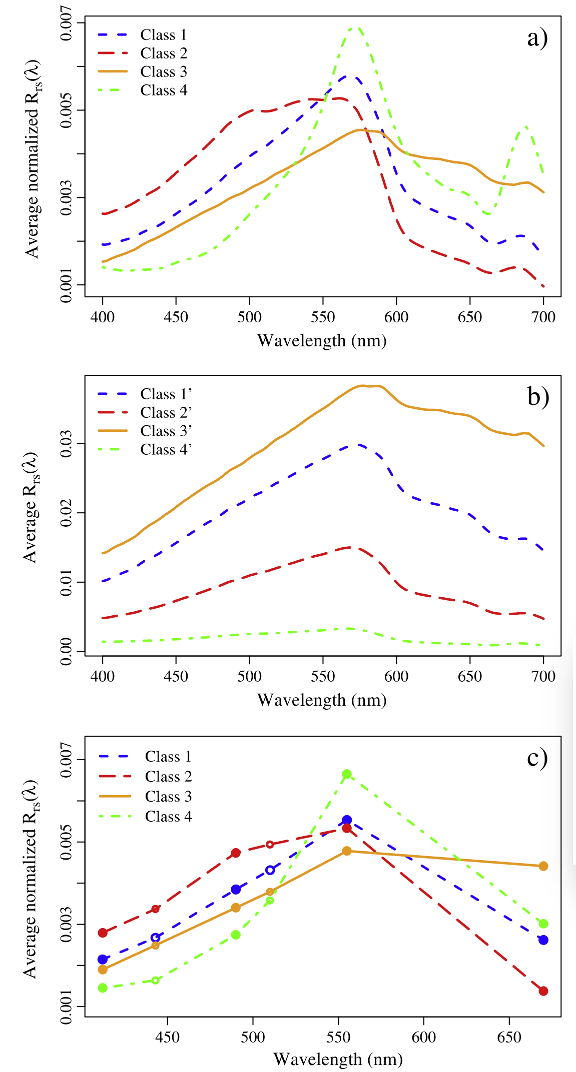

Fig. 3. Average reflectance spectra derived for the Ward's hierarchical classification applied on (a) normalized (Classes 1, 2, 3, 4) and (b) non-normalized (Classes 1′, 2′, 3′, 4′) hyperspectral in situ measurements. Reference spectra obtained from the cluster analysis performed on spectrally normalized reflectance data degraded to the SeaWiFS bands (c) and used to perform the SeaWiFS pixels labeling procedure with selected wavelengths indicated by filled circles. (For interpretation of the references to color in this figure legend, the reader is referred to the web version of this article.)

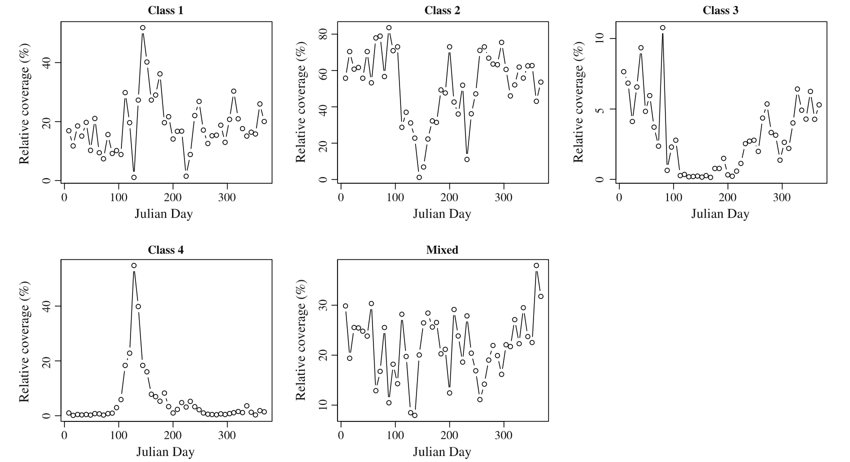

Fig. 9. Annual evolution of the 8-day relative contribution (in %) of the four optical water types and optically mixed waters to the eastern English Channel and Southern North Sea classified turbid waters in 2001.

Contents lists available at SciVerse ScienceDirect

Remote Sensing of Environment

journal homepage: www.elsevier.com/locate/rse

Optical classification of contrasted coastal waters

V. Vantrepotte *, H. Loisel, D. Dessailly, X. Mériaux

INSU-CNRS, UMR 8187, LOG, Laboratoire d'Océanologie et des Géosciences, Université Lille Nord de France, ULCO, 32 avenue Foch, 62930 Wimereux, France

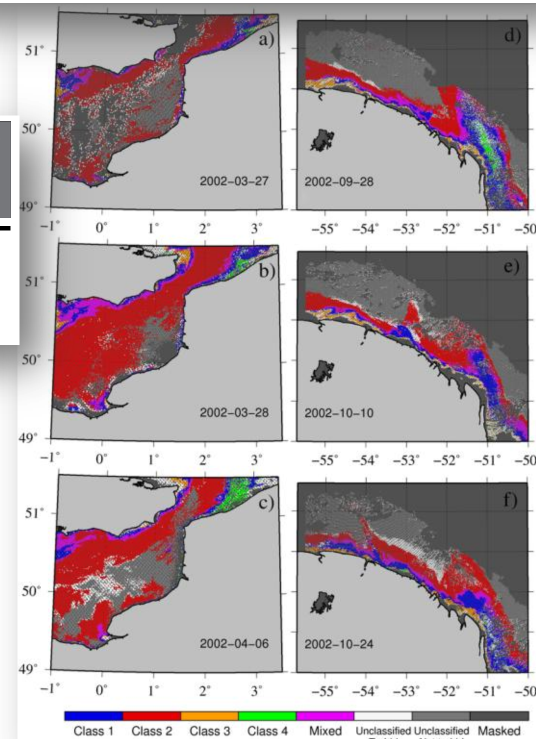

Spectral classification for extreme Case 2 and eutrophic waters

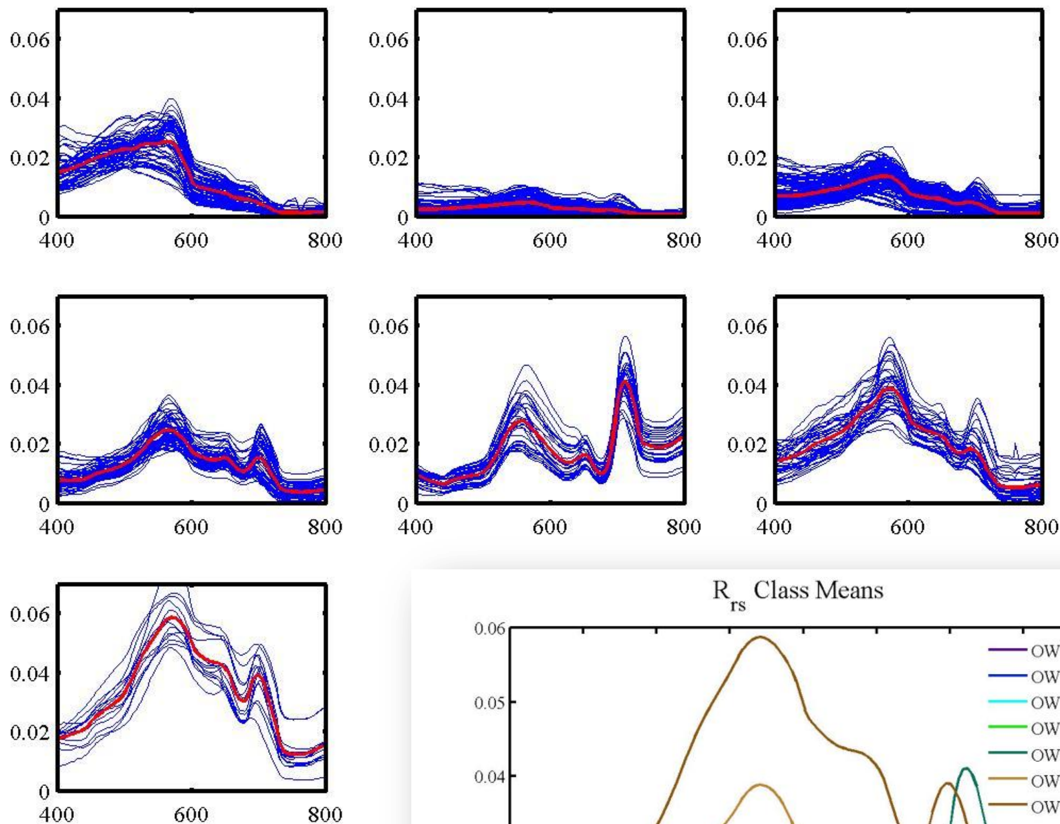

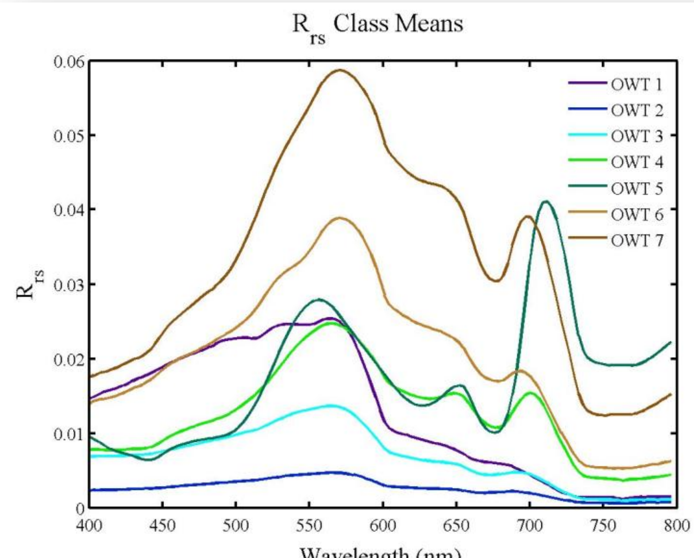

OWT	Chl min	Chl Median	Chl Mean	Chl Max	Std. Dev	N
1	0.53	1.17	1.9	10.75	2.0	50
2	0.40	3.15	7.75	79.4	12.4	114
3	0.63	4.71	13.1	171.9	22.3	133
4	1.42	26,7	31.1	200.0	31.0	70
5	58.7	315.0	295.0	705.0	167.2	32
6	0.45	5.10	15.2	96.6	21.1	38
7	6.84	40.0	40.5	79.7	22.5	13
All						488

Moore et al, in prep

Summary: Suggested Ways Forward for Coastal and Inland Ocean Colour Applications

Measurements

- New instruments, sampling and processing protocols are needed to reduce and quantify errors in validation/algorithm development data and subsequent algorithm products
- Need for autonomous systems, preferably of a low-cost distributed nature, to achieve observations at high enough frequency
- Need for better & more widespread phytoplankton community structure observations to allow better characterisation of diversity, succession etc…..

Bio-Optical Models

- Improvement in bio-optical modelling capabilities to offer effective signal analysis over wide range of optical complexity and phytoplankton communities; and more effective algorithm development and validation.
- Additional benefits would include improved traceability matrices and recommendations for optimal sensor characteristics for eutrophic waters e.g. clusters of narrow bands from green – red – red edge – NIR….

Algorithm Frameworks & Products

- Approaches that offer dynamic and scaleable means of characterisation, algorithm optimisation and error quantification for both synoptic (image-based), and temporal (event- and multi-seasonal scale time series) are needed.
- Spectral classification algorithm structures offer such possibilities in space and time (persistence), with possibilities for regional and application nests, and such approaches should be adopted at least for pilot dissemination.

Networks & Communities

- Global networks of regional ocean colour/observation sites – interact with other communities such as GEO and GEOHAB (GlobalHAB), who have proposed network of global sites acquiring routine, detailed community structure & other data
- Similarly for GEO Blue Planet – integrates OC community into global water quality, ocean information systems, coastal observation, operational ecosystem monitoring, global operational ocean forecasting network, fisheries/aquaculture management systems…

Bring on the global constellation of geostationary ocean colour sensors…..

Assessing the ocean colour signal: sun-induced fluorescence

….a short and uninformed commentary…

- Fluorescence highly variable with dependencies on light history (mixing), physiology, taxonomy…..
- Common qualitative use of MODIS nFLH and MERIS FLH products to reduce ambiguity i.e. to ascertain whether synoptic features are associated with phytoplankton as the sole source of fluorescence at ±683nm
- Quantification of the FLH-type signal using the baseline method becomes difficult in eutrophic waters as backscattering in the red increases
- The presence of sediment/NAP and gelbstoff has considerable effect upon the FLH-type signal, increasing complexity of quantitative use of this signal in coastal waters although some regional algorithms have been developed
- The fluorescence quantum yield is obtainable from semi-analytical type algorithms, and together with phycocyanin fluorescence offers some possibilities for some fluorescence aided PFT recognition……

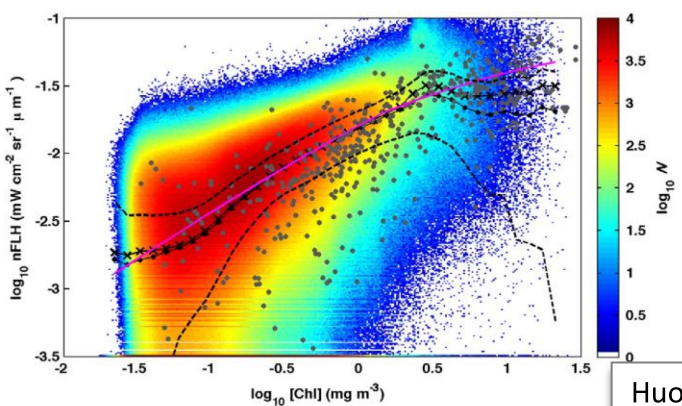

Fig. 1. Relationship between the *nFLH* data product measuring chlorophyll fluorescence at the sea surface and the chlorophyll concentration obtained from the OC2M ocean color algorithm. Black filled circles represent the median of the data falling within equally spaced bins of chlorophyll values extending from half the distance to and from the two adjoining points. The black X's represent the mean of the data for the same interval. The dashed lines represent the median ± the interquartile range. The magenta line is the scaled theoretical model of Huot et al. (2005) for the relationship between *nFLH* and [*chl*] scaled such that it matches the median value of *nFLH* at 0.5 mg chl m^{-3}. The gray points are from the SeaBASS validation dataset for the MODIS AQUA sensor (http://seabass.gsfc.nasa.gov/, accessed 28/10/2010). Colors represent the logarithm in base 10 of the number of points (*N*) within a bin. (For interpretation of the references to color in this figure legend, the reader is referred to the web version of this article.)

Huot et al., 2013

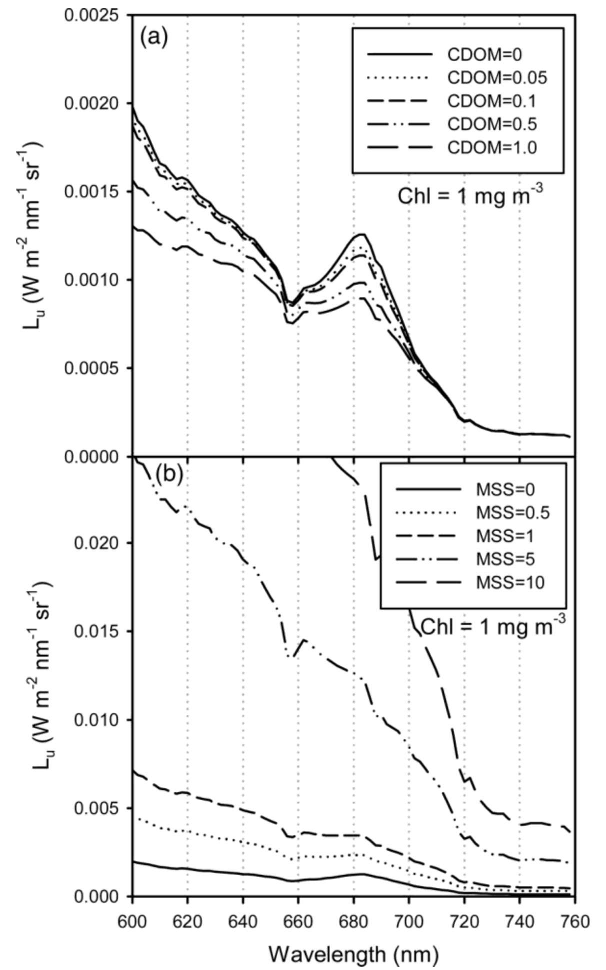

Fig. 8. (a) Effect of increasing CDOM absorption is generally to lower water-leaving radiances in the fluorescence emission waveband. (b) Increasing MSS to 10 g m^{-3} increases background water-leaving radiances by an order of magnitude, and causes the Chl fluorescence peak to become less prominent. Note the order of magnitude difference in y axis scales in panels (a) and (b).

Mckee et al., 2007